

Ekpyrotic Non-Gaussianity – A Review

Jean-Luc Lehnert

*Princeton Center for Theoretical Science,
Princeton University, Princeton, NJ 08544 USA*

*

Ekpyrotic models and their cyclic extensions solve the standard cosmological flatness, horizon and homogeneity puzzles by postulating a slowly contracting phase of the universe prior to the big bang. This ekpyrotic phase also manages to produce a nearly scale-invariant spectrum of scalar density fluctuations, but, crucially, with significant non-gaussian corrections. In fact, some versions of ekpyrosis are on the borderline of being ruled out by observations, while, interestingly, the best-motivated models predict levels of non-gaussianity that will be measurable by near-future experiments. Here, we review these predictions in detail, and comment on their implications.

Contents

I. Motivation and Introduction	2
II. Ekpyrotic and Cyclic Cosmology	4
III. Linear Perturbations	13
A. Single Scalar Field	13
B. Two Fields: the Entropic Mechanism	17
IV. Higher-Order Perturbations and Predictions for Non-Gaussianity	23
A. Definitions and Local Non-Gaussianity	23
B. Generation of Entropy Perturbations	26
C. Ekpyrotic Conversion	27
D. Kinetic Conversion	30
V. Discussion of the Results	35
Acknowledgments	37
References	37

*Electronic address: jlehnert@princeton.edu

I. MOTIVATION AND INTRODUCTION

The standard big bang cosmology is hugely successful in describing the evolution of our universe from the time of nucleosynthesis onwards. However, a central assumption is that the universe started out in a hot big bang, and in a special state: extrapolating back from current knowledge, we know that early on the universe must have been very flat, homogeneous and isotropic, with in addition small density perturbations with a nearly scale-invariant spectrum and a nearly gaussian distribution. Hence, the “initial” state of the universe was far from random, and its specialness prompts us to try and explain it via a dynamical mechanism.

The most studied such mechanism is the model of inflation, which assumes that there was a phase of rapid, accelerated expansion preceding the hot big bang; for a comprehensive review see [1]. Such a phase can be modeled by having a scalar field (the “inflaton”) with a positive and suitably flat potential. Inflation has the property of flattening the universe, so that, if it lasts long enough, the flatness of the “initial” state can be explained. Moreover, inflation possesses the remarkable byproduct that it generates nearly scale-invariant spectra of scalar and tensor perturbations by amplifying quantum fluctuations. The predicted scalar perturbations are in excellent agreement with current observations, but the tensor perturbations have yet to be observed - their discovery would be a strong indication for the correctness of the inflationary picture. However, inflation also presents a number of conceptual problems: for example, even though the inflationary phase is supposed to erase all memory of initial conditions, this is not really the case. In order for inflation to start in a given patch of space, that patch must be reasonably smooth over several Planck lengths and the inflaton field must have a small initial velocity (the “patch” and “overshoot” problems respectively, see *e.g.* [1, 2]). Also, it has been realized not long ago that inflation is geodesically incomplete towards the past, which means that the predictions of the theory depend on the specification of data on a spacelike initial hypersurface [3]. In other words, inflation requires its own initial conditions. Hence, if inflation is correct, it will only form a part of the story. More worrying is the problem of unpredictability, which is associated with the quantum nature and the effectiveness of inflation. Inflation ends when the inflaton field oscillates around a minimum of its potential, and “reheats” the universe by decaying into standard model particles. However, for generic initial conditions there will always be regions in which rare but large quantum fluctuations kick the inflaton field back up its potential and keep a fraction of the universe in the inflationary phase. In most of the concrete realizations of inflation, the region that keeps inflating expands so fast that it quickly dominates the overall volume of the universe. Hence, inflation never ends

and the global picture of this process of “eternal inflation” is that of an empty de Sitter universe punctured by an infinite number of small pockets where inflation has ended (at a random time) [4]. Because inflation ends at a random moment in these pocket universes, the pockets might have become sufficiently flattened or not, they might have acquired scale-invariant perturbations or not. Without a measure which would determine the relative likelihood of the various pockets, it becomes difficult to know exactly what eternal inflation predicts! These problems do not mean that the idea of inflation is wrong, but, if inflation continues to be supported by observations, they will have to be addressed. In the meantime, the seriousness of these open problems means that it is worthwhile considering alternative models for the early universe in parallel.

The present review deals with one such model in particular, namely the ekpyrotic model and its extension, the cyclic universe; for a comprehensive overview see [5]. In this model, the inflationary phase is replaced by the ekpyrotic phase, which is a slowly contracting phase preceding the big bang. The ekpyrotic phase can be modeled by having a scalar field with a negative and steep potential. As described in detail below, it also manages to flatten a given region of the universe, and generates nearly scale-invariant scalar perturbations, but no observable tensor fluctuations. At the linear level, the scalar fluctuations are virtually indistinguishable from the perturbations produced by inflation, but at higher orders the predictions differ. Since primordial gravitational waves might turn out to be rather elusive to measure over the coming years, the most promising way of distinguishing between alternative models of the early universe is therefore by studying these higher-order, non-gaussian signatures.

There is a simply, intuitive argument for why the predictions regarding higher-order corrections to the linear perturbations should differ for models of inflation and ekpyrosis. For a scalar field fluctuation $\delta\varphi$, the semi-classical probability density is roughly given by $e^{-S_E(\delta\varphi)}$, where $S_E(\delta\varphi)$ is the euclidean action [6]. Since inflation requires a very flat potential, the inflaton is an almost free field. For a free field, the action is quadratic in the field, and hence the probability distribution is simply a gaussian distribution. For an exact gaussian distribution the 3-point function $\langle\delta\varphi^3\rangle$ vanishes, and hence for inflation, where the field is almost free, we would expect the 3-point function to be non-zero, but small. For ekpyrosis, on the other hand, the potential is steep, and hence the scalar field is necessarily significantly self-coupled. This has the consequence that ekpyrotic models generally predict significant levels of non-gaussianity. In fact, some versions of ekpyrosis are already on the borderline of being ruled out by observations, while the best-motivated models predict values that are measurable by near-future experiments. Thus, the non-gaussian predictions are crucial in assessing the viability of various cosmological models, and promise to significantly enhance our

understanding of the physics of the early universe.

The plan of this review is to start with a brief summary of the main ideas behind ekpyrotic and cyclic models of the universe. We will then discuss in some detail the generation of linear cosmological perturbations (a good understanding of the linear perturbations greatly facilitates an understanding of the higher-order ones), before turning to the main subject of the review, namely the non-gaussian corrections to these linear perturbations. We will conclude with a discussion of the non-gaussian predictions and in particular their observability and relation to current observational limits, as well as the consequences of a potential detection.

II. EKPYROTIC AND CYCLIC COSMOLOGY

The ekpyrotic phase is the cornerstone of ekpyrotic and cyclic models of the universe: it is a conjectured, slowly contracting phase preceding the big bang, and it resolves the standard cosmological puzzles [7, 8]. The main feature of ekpyrosis is that during this phase the equation of state

$$w \equiv \frac{p}{\rho} \gg 1 \quad (1)$$

is very large (here p and ρ denote the average pressure and energy density of the universe). Let us briefly explore the most direct consequences of such an ultra-stiff equation of state. Consider a Friedmann-Robertson-Walker (FRW) metric¹

$$ds^2 = -dt^2 + a(t)^2 \left(\frac{dr^2}{1 - \kappa r^2} + r^2 d\Omega_2^2 \right) \quad (2)$$

where $a(t)$ denotes the scale factor of the universe and $\kappa = -1, 0, 1$ for an open, flat or closed universe respectively. If the universe is filled with a number of fluids interacting only via gravity and with energy densities ρ_i and constant equations of state w_i , then the equations of continuity

$$\dot{\rho}_i + 3\frac{\dot{a}}{a}(\rho_i + p_i) = 0 \quad (3)$$

(where dots denote derivatives with respect to time t) imply that they will evolve according to

$$\rho_i \propto a^{-3(1+w_i)}. \quad (4)$$

The Einstein equations for this system contain a constraint equation, better known as the Friedmann equation, which involves the Hubble parameter $H \equiv \dot{a}/a$:

$$H^2 = \frac{1}{3} \left(\frac{-3\kappa}{a^2} + \frac{\rho_{m,0}}{a^3} + \frac{\rho_{r,0}}{a^4} + \frac{\rho_{a,0}}{a^6} + \dots + \frac{\rho_{\phi,0}}{a^{3(1+w_\phi)}} \right). \quad (5)$$

¹ I will mostly use natural units $\hbar = c = 1$ and $8\pi G = M_{Pl}^{-2} = 1$.

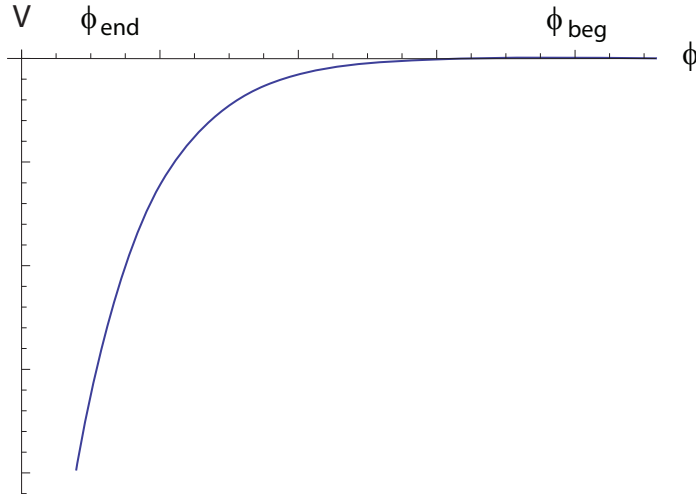


FIG. 1: The potential during ekpyrosis is negative and steeply falling; it can be modeled by the exponential form $V(\phi) = -V_0 e^{-c\phi}$.

The $\rho_{i,0}$ s are constants giving the energy densities at scale factor $a = 1$ of the various constituents of the universe: we consider the universe to be composed of non-relativistic matter (subscript m), radiation (r) and the energy density associated with anisotropies in the curvature of the universe (a). In addition, we consider there to be ekpyrotic (scalar) matter, denoted by the subscript ϕ , and, as usual, there is a contribution due to the average curvature of space.

As the universe contracts, components whose energy density scales with a higher negative power of the scale factor a will successively come to dominate, first matter, then radiation, then anisotropies and eventually, since $w_\phi \gg 1$ by assumption, the ekpyrotic matter. This means that the relative energy densities in curvature and anisotropies, for example, become smaller and smaller, the longer the ekpyrotic contracting phase lasts. In other words, if ekpyrosis lasts long enough, the flatness problem is solved. We will make this statement quantitative below. Strictly speaking, for the flatness problem to be solved, all we need is a matter component with $w > 1$. In the next section, we will see that for realistic ekpyrotic models, typically $w_\phi \gg 1$. In passing, we should also point out that there is no horizon problem in ekpyrotic and cyclic models, as there is plenty of time before the big bang for different parts of our currently observable universe to have been in causal contact with each other.

But what form of matter can have the large equation of state that we require? A simple way to model the ekpyrotic matter is to have a scalar field ϕ with a steep and negative potential $V(\phi)$.

A concrete example is provided by the negative exponential

$$V(\phi) = -V_0 e^{-c\phi}, \quad (6)$$

where V_0 and c are constants - see Fig. 1. In the context of string theory, such scalar fields appear very naturally, and the ekpyrotic potential can then correspond to an attractive force between branes - this picture will be briefly described below.

Given an explicit form of the potential, such as (6), we can solve for the evolution of the universe. In fact it is straightforward to generalize the treatment to having many scalars ϕ_i with potentials $V_i(\phi_i)$. Then, in a flat FRW background and neglecting other matter components, the equations of motion become

$$\ddot{\phi}_i + 3H\dot{\phi}_i + V_{i,\phi_i} = 0 \quad (7)$$

and

$$H^2 = \frac{1}{3} \left[\frac{1}{2} \sum_i \dot{\phi}_i^2 + \sum_i V_i(\phi_i) \right], \quad (8)$$

where $V_{i,\phi_i} = (\partial V_i / \partial \phi_i)$ with no summation implied. If all the fields have negative exponential potentials $V_i(\phi_i) = -V_i e^{-c_i \phi_i}$ and if $c_i \gg 1$ for all i , then the Einstein-scalar equations admit the *scaling solution*

$$a = (-t)^{1/\epsilon}, \quad \phi_i = \frac{2}{c_i} \ln(-\sqrt{c_i^2 V_i / 2t}), \quad \frac{1}{\epsilon} = \sum_i \frac{2}{c_i^2}. \quad (9)$$

Thus, we have a very slowly contracting universe with (constant) equation of state

$$w \equiv \frac{\sum_i \frac{1}{2} \dot{\phi}_i^2 - V_i(\phi_i)}{\sum_j \frac{1}{2} \dot{\phi}_j^2 + V_j(\phi_j)} = \frac{2\epsilon}{3} - 1 \gg 1. \quad (10)$$

We are using a coordinate system in which the big crunch occurs at $t = 0$; in other words, the time coordinate is negative during the ekpyrotic phase. Here, the parameter ϵ corresponds to the *fast-roll* parameter and is typically of $\mathcal{O}(100)$; its definition is identical with that in inflation, where its value is typically of $\mathcal{O}(1/100)$ and where, correspondingly, it is called the *slow-roll* parameter.

Using this explicit solution, we can get an idea for how long the ekpyrotic phase has to last in order for the flatness problem to be solved. Quantitatively, the problem can be formulated as follows: dividing the Friedmann equation (5) by H^2 we can see that the fractional energy density stored in the average curvature of the universe is given by

$$\frac{\kappa}{(aH)^2}. \quad (11)$$

At the present time, observations imply that this quantity is smaller than 10^{-2} in magnitude [9]. If we assume a radiation-dominated universe, which is a good approximation for this calculation, then $aH \propto t^{-1/2}$ and hence, if we extrapolate back to the Planck time, the fractional energy density in curvature must have been smaller than

$$\frac{t_{Pl}}{t_0} 10^{-2} \approx 10^{-62}, \quad (12)$$

an incredibly small number. However, from (9), we can see that during the ekpyrotic phase the scale factor a remains almost constant, while the Hubble parameter $H \propto t^{-1}$. Hence aH grows by a factor of 10^{30} as long as

$$|t_{ek-beg}| \geq e^{60} |t_{ek-end}|, \quad (13)$$

where the subscripts $ek - beg$ and $ek - end$ refer to the beginning and the end of the ekpyrotic phase respectively. As will be discussed in the next section, we need $t_{ek-end} \approx -10^3 M_{Pl}^{-1}$ in order to obtain the observed amplitude of cosmological perturbations, so that we need

$$|t_{ek-beg}| \geq 10^{33} M_{Pl}^{-1} = 10^{-10} s. \quad (14)$$

This is the minimum time the ekpyrotic phase has to last in order to solve the flatness problem. Cosmologically speaking, this is a very short time, attesting to the effectiveness of the ekpyrotic phase.

Before discussing the cosmological perturbations produced during the ekpyrotic phase, it is useful to provide a quick overview of how the ekpyrotic phase might fit into a more complete cosmological model. The crucial ingredient in any such model is the proposed mechanism for how the ekpyrotic contracting phase (with $H < 0$) and the subsequent radiation-dominated expanding phases (with $H > 0$) should link up. The Einstein equations provide the relation

$$\dot{H} = -\frac{1}{2}(\rho + p). \quad (15)$$

All forms of matter that are currently known to exist obey the *null energy condition*

$$\rho + p \geq 0 \quad (\text{NEC}), \quad (16)$$

which implies $\dot{H} \leq 0$ and which thus precludes a smooth transition between a contracting and an expanding universe. This leaves two possibilities for achieving such a transition: either the NEC is violated during the transition, or the transition is classically singular.

In *new ekpyrotic* models [10–12], a smooth reversal from contraction to expansion is achieved by adding a further matter component to the universe which can violate the NEC. The particular

example that these models consider is the so-called ghost condensate, which corresponds to the gravitational equivalent of a Higgs phase [13]. It is not clear yet whether or not the ghost condensate can be obtained from a fundamental theory such as string theory [14] (in the more restricted framework of quantum field theory it seems impossible to construct a stable ghost condensate model [15]); however, it is interesting that string theory contains many objects (orientifolds, negative-tension branes) which do violate the NEC. Of course, simply adding such a component is not enough: it must become relevant as the universe contracts, and vanish again as the universe expands. The simplest way in which to achieve this is by assuming that the ghost condensate itself also plays the role of the ekpyrotic matter, and that after the transition to expansion, it decays into ordinary matter fields. This scenario requires the ghost condensate to possess both a particular form for its kinetic term and a particular potential; for details regarding possible realizations see [10, 12].

The *cyclic* model of the universe [16, 17] is based on the braneworld picture of the universe, in which spacetime is effectively 5-dimensional, but with one dimension not extending indefinitely, but being a line segment, see Fig. 2. The endpoints of this line segment (orbifold) are two $(3+1)$ -dimensional boundary branes. In the full string theory setup, there is in addition a 6-dimensional internal manifold at each point in the 5-dimensional spacetime, for a total of 11 dimensions [18]. This description of the universe stems from string theory, and in particular the duality, known as *Hořava-Witten theory* [19], between 11-dimensional supergravity and the $E_8 \times E_8$ heterotic string theory. All matter and forces, except for gravity, are localized on the branes, while gravity can propagate in the whole spacetime. Our universe, as we see it, is identified with one of the boundary branes and, as long as the branes are far apart, can interact with the other brane only via gravity. The cyclic model assumes that there is an attractive force between the two branes, which causes the branes to approach each other. This force is modeled by a potential of the form shown in Fig. 3. Note that the potential incorporates an ekpyrotic part. From the higher-dimensional point of view, the ekpyrotic phase has the rather non-intuitive property that it flattens the branes to a very high degree. Eventually the two branes collide and bounce off each other. It is this collision that, from the point of view of someone living on one of the branes, looks like the big bang. Classically, the collision is singular, as the orbifold dimension shrinks to zero size. The collision is slightly inelastic and produces matter and radiation on the branes, where the standard cosmological evolution now takes place. However, due to quantum fluctuations, the branes are slightly rippled and do not collide everywhere at exactly the same time. In some places, the branes collide slightly earlier, which means that the universe has a little bit more time to expand and cool. In other places,

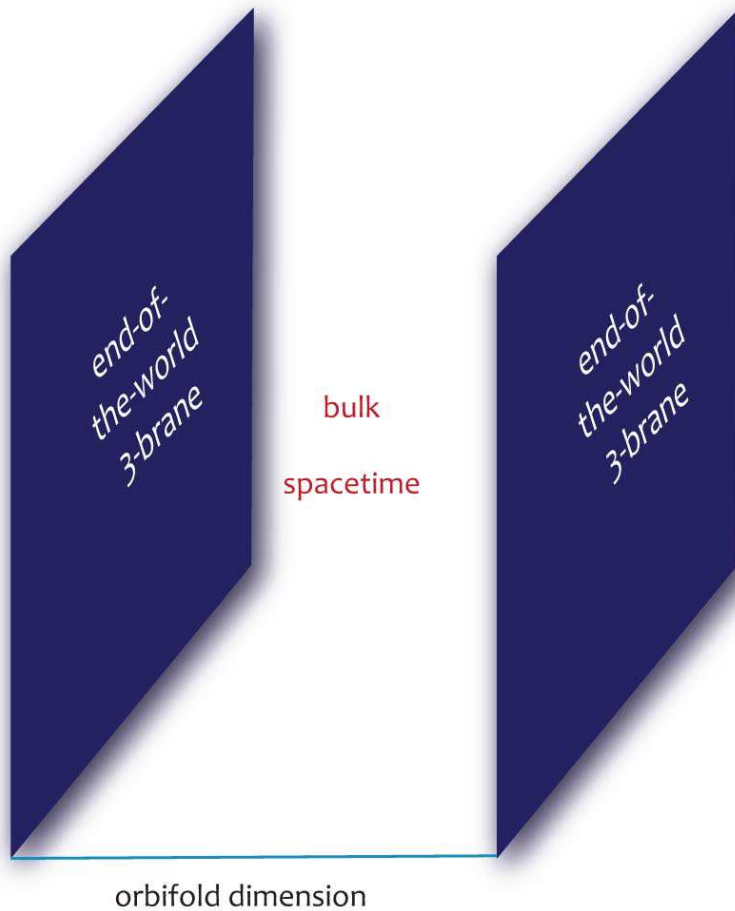


FIG. 2: The braneworld picture of our universe. Think of a sandwich: the 5-dimensional bulk spacetime is bounded by two 4-dimensional boundary branes. There is no space “outside” of the sandwich, but the branes can be infinite in all directions perpendicular to the line segment (orbifold). In the M-theory embedding, there are 6 additional internal dimensions at each point of the sandwich.

the collision takes place slightly later, and those regions remain a little hotter. This provides a heuristic picture of the way temperature fluctuations are naturally produced within the model. Shortly after the branes have separated, the distance between the boundary branes gets almost stabilized, but the branes start attracting each other again very slightly. This very slight attraction acts as quintessence, and is identified with the dark energy observed in the universe. After a long time, and as the branes become closer again, they start attracting each other more strongly so that we get another ekpyrotic phase and eventually another brane collision with the creation of new matter. In this way, a cyclic model of the universe emerges. Before continuing, we should mention the main open issues related to the cyclic model: the first one concerns the potential, which at this point is simply conjectured. It will be important to see if a potential of the required shape

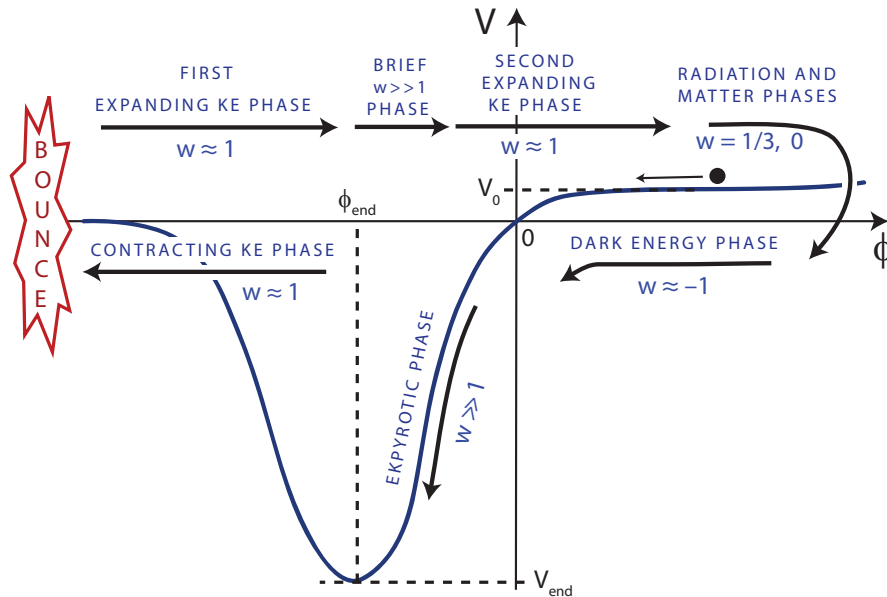


FIG. 3: The potential for the cyclic universe integrates the ekpyrotic part and a quintessence epoch, but is irrelevant at the brane collision. A possible form for the potential is $V(\phi) = V_0(e^{b\phi} - e^{-c\phi})F(\phi)$, with $b \ll 1$, $c \gg 1$ and $F(\phi)$ tends to unity for $\phi > \phi_{end}$ and to zero for $\phi < \phi_{end}$. Reproduced with permission from [8].

can be derived from microphysics. And the second is the brane collision, which so far has been extensively studied at the classical and semi-classical level [20], but a full quantum treatment has remained elusive.

In the discussion above, we have mostly focussed on models involving one effective scalar field. However, there are two good reasons to extend the analysis to two or more scalars: first, in embedding the ekpyrotic and cyclic models in M-theory, there are two universal scalars, namely the radion mode (which determines the distance between the branes) and the volume modulus of the internal 6-dimensional manifold [21]. There can be many more scalar fields (such as the shape moduli of the internal space), but we always must consider these two universal scalars. And secondly, as we will see in the next section, it is much more natural to generate a nearly scale-invariant spectrum of curvature perturbations (in agreement with observations) in models with two scalars than in models with only one. However, multi-field ekpyrotic models present some qualitatively new features, which we discuss briefly here.

The 4-dimensional effective action

$$S = \int \sqrt{-g} [R - \frac{1}{2}(\partial\phi_1)^2 - \frac{1}{2}(\partial\phi_2)^2 - V(\phi_1, \phi_2)] \quad (17)$$

can be obtained as the low-energy limit of Hořava-Witten theory, where ϕ_1 and ϕ_2 are related by a field redefinition to the radion and the internal volume modulus [22]. We are assuming that during the ekpyrotic phase, both fields feel an ekpyrotic-type potential, *e.g.*

$$V(\phi_1, \phi_2) = -V_1 e^{-c_1 \phi_1} - V_2 e^{-c_2 \phi_2}. \quad (18)$$

Then it is much more natural to discuss the dynamics in terms of the new variables σ and s pointing transverse and perpendicular to the field velocity respectively [23, 24]; they are defined, up to unimportant additive constants which we will fix below, via

$$\sigma \equiv \frac{\dot{\phi}_1 \phi_1 + \dot{\phi}_2 \phi_2}{\dot{\sigma}}, \quad s \equiv \frac{\dot{\phi}_1 \phi_2 - \dot{\phi}_2 \phi_1}{\dot{\sigma}}, \quad (19)$$

with $\dot{\sigma} \equiv (\dot{\phi}_1^2 + \dot{\phi}_2^2)^{1/2}$. It is also useful to define the angle θ of the trajectory in field space, via [25]

$$\cos \theta = \frac{\dot{\phi}_1}{\dot{\sigma}}, \quad \sin \theta = \frac{\dot{\phi}_2}{\dot{\sigma}}. \quad (20)$$

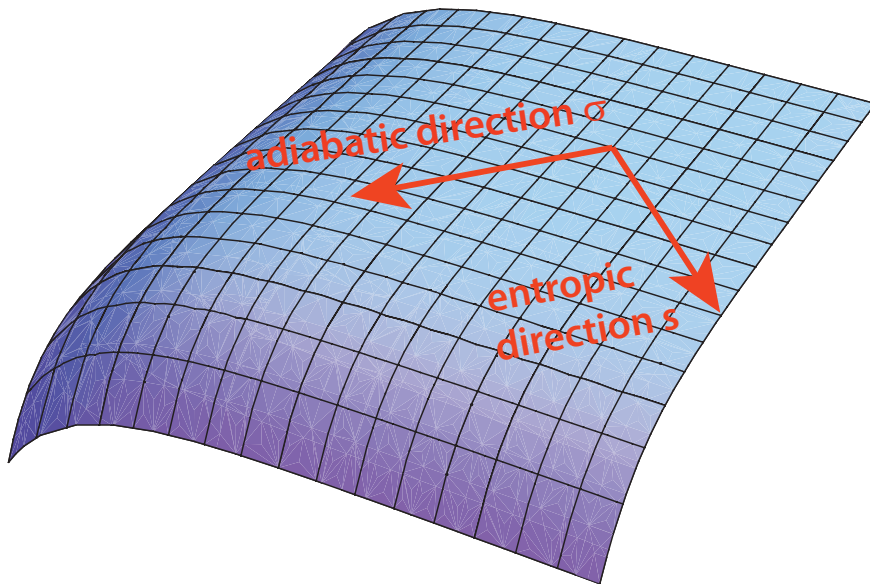


FIG. 4: After a rotation in field space, the two-field ekpyrotic potential can be viewed as composed of an ekpyrotic direction (σ) and a transverse tachyonic direction (s). The ekpyrotic scaling solution corresponds to motion along the ridge of the potential. Perturbations along the direction of the trajectory are adiabatic/curvature perturbations, while perturbations transverse to the trajectory are entropy/isocurvature perturbations.

In terms of these new variables, the potential can be re-expressed as

$$V_{ek} = -V_0 e^{\sqrt{2\epsilon}\sigma} \left[1 + \epsilon s^2 + \frac{\kappa_3}{3!} \epsilon^{3/2} s^3 + \frac{\kappa_4}{4!} \epsilon^2 s^4 + \dots \right], \quad (21)$$

where for exact exponentials of the form (18), one has $\kappa_3 = 2\sqrt{2}(c_1^2 - c_2^2)/|c_1 c_2|$ and $\kappa_4 = 4(c_1^6 + c_2^6)/(c_1^2 c_2^2 (c_1^2 + c_2^2))$. However, in the absence of a microphysical derivation of the potential, we will simply take $\kappa_3, \kappa_4 \sim \mathcal{O}(1)$ and express all results in terms of κ_3, κ_4 . See also Fig. 4 for an illustration of the potential. The ekpyrotic scaling solution becomes

$$a(t) = (-t)^{1/\epsilon} \quad \sigma = -\sqrt{\frac{2}{\epsilon}} \ln \left(-\sqrt{\epsilon V_0 t} \right) \quad s = 0, \quad (22)$$

with the angle θ being constant. The solution corresponds to motion along a ridge in the potential, as is evident from the figure. Hence, in contrast to the single field case, the multi-field ekpyrotic background evolution is unstable to small perturbations [26, 27]. This implies that the trajectory must be localized near the ridge with extreme precision at the beginning of the ekpyrotic phase, the condition being that the field should stray no more than a value of e^{-60} (at best) in Planck units from the ridge at the beginning of ekpyrosis [11]. Thus, at first sight, it looks as if the multi-field ekpyrotic phase has not managed to solve the problem of initial conditions. However, there currently exist two approaches addressing this issue: the authors of [11] considered the existence of a “pre-ekpyrotic” phase during which the potential is curved upwards and during which the trajectory is localized. Meanwhile, in the context of the cyclic universe, there is a natural resolution of the issue of initial conditions, not involving any new ingredients of the model: indeed, the multi-field cyclic universe *selects* those regions that happen to correspond to trajectories sufficiently close to the ridge, in the sense that these regions are vastly amplified over the course of one cycle due to the phases of radiation, matter and dark energy domination (note that the ekpyrotic phase shrinks the universe by a negligible amount). At the same time, the regions corresponding to trajectories not sufficiently close to the ridge (this would include the vast majority of trajectories) do not undergo a full ekpyrotic phase, and after these regions undergo chaotic mixmaster behavior close to the big crunch, they simply collapse (presumably they will end up forming black holes) and stop both growing and cycling. In this way the global structure of the universe becomes of the *phoenix* type, in which vast habitable regions are interspersed with small collapsed ones. The important point is that the habitable regions, which are the only regions of interest to us here, automatically correspond to the regions that had the right “initial conditions” at the beginning of their preceding ekpyrotic phase. This is discussed in detail in [28]; see also the essay [29].

III. LINEAR PERTURBATIONS

A. Single Scalar Field

In the last section, we have dealt with the classical evolution during the ekpyrotic phase. We will now add quantum fluctuations and we will see that, just as in inflation, the quantum fluctuations get amplified into classical density perturbations. Hence, on top of resolving the standard cosmological puzzles, the ekpyrotic phase can also be the source of the primordial temperature fluctuations whose imprint is seen in maps of the cosmic microwave background, provided that the amplitude and spectrum of the fluctuations match observations.

From the study of inflationary models, we have developed the intuition that quantum fluctuations that get stretched to super-horizon scales turn into classical perturbations, roughly speaking because the fluctuations go out of causal contact with themselves, do not remember locally that they are in fact fluctuations and end up as local, classical perturbations to the background evolution. In inflation, this effect occurs because the horizon is approximately constant in size while the wavelengths of the quantum modes get stretched exponentially with time (the scale factor of the universe grows exponentially). For ekpyrosis, the scaling solution (9) shows that the scale factor is almost constant, so that the mode wavelengths remain almost constant too. However, the horizon, which is proportional to $1/H \sim t$, shrinks rapidly as $t \rightarrow 0$ and hence the modes automatically become of super-horizon size². We will now discuss in some detail what amplitude and spectrum these modes obtain. We will first concentrate on the single field case, before discussing two fields.

Since the scale factor evolves very little during the ekpyrotic phase, one is tempted to simply turn gravity off as a first approximation, and to consider the theory consisting only of a scalar field with a steep and negative potential [32]:

$$S = \int d^4x \left[-\frac{1}{2}(\partial\phi_1)^2 + V_1 e^{-c_1\phi_1} \right]. \quad (23)$$

Then, if we define scalar fluctuations $\delta\phi$ via $\phi_1 \equiv \bar{\phi}_1(t) + \delta\phi(t, \underline{x})$, where $\bar{\phi}_1 = \frac{2}{c_1} \ln(-\sqrt{c_1^2 V_1/2t})$ denotes the background evolution, the equation of motion for the fluctuations is given by

$$\delta\ddot{\phi} - \nabla^2\delta\phi + V_{,\phi_1\phi_1}\delta\phi = 0, \quad (24)$$

² Since tensor modes/gravitational waves depend on the evolution of the scale factor alone, and since the scale factor shrinks imperceptively slowly during ekpyrosis, there are no substantial gravity waves produced during the ekpyrotic phase (the background spacetime is almost Minkowski!) [30]. In fact, the dominant gravitational waves that are produced from ekpyrosis are those that arise from the backreaction of the scalar fluctuations onto the metric, at second order in perturbation theory [31].

where $V_{,\phi_1\phi_1} = -2/t^2$. We then expand the fluctuation field $\delta\phi$ into Fourier modes

$$\delta\phi = \int \frac{d^3k}{(2\pi)^3} a_{\mathbf{k}} \chi_k e^{i\mathbf{k}\cdot\mathbf{x}} + h.c. \quad (25)$$

where the χ_k s are the positive frequency mode functions (due to the assumed cosmological symmetries, they depend only on the magnitude $k = |\mathbf{k}|$). We proceed to quantize the field by imposing the canonical commutation relations

$$[a_{\mathbf{k}}, a_{\mathbf{k}'}] = [a_{\mathbf{k}}^\dagger, a_{\mathbf{k}'}^\dagger] = 0, \quad [a_{\mathbf{k}}, a_{\mathbf{k}'}^\dagger] = (2\pi)^3 \delta(\mathbf{k} - \mathbf{k}') \quad (26)$$

In the process, the $a_{\mathbf{k}}$ s have been promoted to (annihilation) operators, and the vacuum state $|0\rangle$ is defined by $a_{\mathbf{k}}|0\rangle = 0$. The mode functions obey the equation of motion

$$\ddot{\chi}_k + k^2 \chi_k - \frac{2}{t^2} \chi_k = 0, \quad (27)$$

which admits the two solutions $\chi_k \propto e^{-ikt}(1 - \frac{i}{kt}), e^{ikt}(1 + \frac{i}{kt})$. However, as $t \rightarrow -\infty$ the modes should asymptote to the Minkowski space free particle state $\chi_k \rightarrow e^{-ikt}/\sqrt{2k}$ (note that in that limit (27) reduces to the equation of a simple harmonic oscillator), and this fixes the solution to be

$$\chi_k = \frac{1}{\sqrt{2k}} e^{-ikt} \left(1 - \frac{i}{kt}\right). \quad (28)$$

Towards the end of the ekpyrotic phase, we have $|kt| \ll 1$, and then the solution can be well approximated by

$$\chi_k \approx \frac{-i}{\sqrt{2}k^{3/2}t}. \quad (29)$$

The quantum fluctuations have a mean that is zero, $\langle 0|\delta\phi|0\rangle = 0$. However, the *variance* $\Delta_\phi^2(k)$, which is defined by $\langle 0|\delta\phi^2|0\rangle \equiv \int \frac{dk}{k} \Delta_\phi^2(k)$, does not vanish. It is conventional to write the variance as

$$\Delta_\phi^2(k) = \Delta_\phi^2(k_0) \left(\frac{k}{k_0}\right)^{n_s-1}, \quad (30)$$

where k_0 denotes a reference scale and n_s is the *spectral index*.

A related concept in momentum space is the *power spectrum* $P(k)$, defined by

$$P(k) \equiv |\chi_k|^2 = \frac{2\pi^2}{k^3} \Delta_\phi^2(k). \quad (31)$$

It is the Fourier transform of the 2-point correlation function, and we can equivalently define it as

$$\langle \zeta_{\mathbf{k}} \zeta_{\mathbf{k}'} \rangle \equiv (2\pi)^3 P(k) \delta^3(\mathbf{k} + \mathbf{k}') \quad (32)$$

where isotropy dictates that P only depends on $k = |\mathbf{k}|$. We will find this definition useful later on.

In our case, we have that at late times

$$\langle 0|\delta\phi^2|0\rangle = \int \frac{d^3k}{(2\pi)^3} \chi_k^* \chi_k = \int \frac{4\pi k^2 dk}{(2\pi)^3} \frac{1}{2k^3 t^2}, \quad (33)$$

so that the variance is given by

$$\Delta_\phi^2(k) = \frac{1}{4\pi^2 t^2} \quad \rightarrow \quad n_s = 1. \quad (34)$$

The variance is independent of k , and hence we obtain a scale-invariant spectrum for $\delta\phi$. This looks very promising! However, we really must include gravity in our analysis, and calculate the spectrum for the curvature perturbation ζ , which is the quantity that is measured to have a nearly scale-invariant spectrum of perturbations.

Once we add gravity, it is easiest to perform the calculation in so-called ζ -gauge, where the perturbations in the scalar field are gauged away and all perturbations are expressed via dilatations of the 3-metric:

$$\delta\phi = 0 \quad (35)$$

$$ds^2 = -dt^2 + a^2(t)e^{2\zeta(t,\mathbf{x})} dx_j dx^j, \quad (36)$$

where $j = 1, 2, 3$. Then, using the background scaling solution (9), the action reduces to an action for ζ which is given by [33]

$$S = - \int \epsilon g^{\mu\nu} \partial_\mu \zeta \partial_\nu \zeta. \quad (37)$$

During ekpyrosis, ϵ is typically nearly constant. In fact, in the scaling solution used above, we have already made the approximation that ϵ is constant, and with this approximation, the equation of motion for ζ resulting from the action above is particularly simple: in Fourier space it is given by

$$\ddot{\zeta}_k + 3H\dot{\zeta}_k + \frac{k^2}{a^2}\zeta_k = 0. \quad (38)$$

If we use conformal time τ , defined via $dt \equiv a d\tau$, and the notation $' \equiv \frac{d}{d\tau}$, the above equation becomes

$$\zeta_k'' + 2\frac{a'}{a}\zeta_k' + k^2\zeta_k = 0. \quad (39)$$

After a further change of variables to $y \equiv a\zeta/\sqrt{-k\tau}$ and $x \equiv -k\tau$, the equation turns into a Bessel equation $x^2 \frac{d^2 y}{dx^2} + x \frac{dy}{dx} + (x^2 - \alpha^2)y = 0$, with $\alpha = \sqrt{\tau^2 a''/a + 1/4} \approx 1/2$ since $a \approx \text{constant}$. Hence

the solutions are given by the Hankel functions $y \propto H_{1/2}^{(1)}(-k\tau), H_{1/2}^{(2)}(-k\tau)$ and with the boundary condition that we want $\zeta \rightarrow e^{-ik\tau}/\sqrt{2k}$ as $\tau \rightarrow -\infty$, we obtain the solution (up to a phase)³

$$\zeta = \frac{\sqrt{-\tau}}{a} H_{1/2}^{(1)}(-k\tau). \quad (40)$$

At late times, the variance becomes

$$\langle 0|\zeta^2|0\rangle = \int \frac{d^3k}{(2\pi)^3} \frac{(-\tau)}{a^2} |H_{1/2}^{(1)}(-k\tau)|^2 \sim \int \frac{dk}{k} k^2, \quad (41)$$

and hence we get a spectral index $n_s = 3$. This spectrum is *blue*, as there is more power on smaller scales, and it is in disagreement with observations [32–34]. Hence, the scale-invariant spectrum of the scalar perturbation in the no-gravity theory did not get transferred to the curvature perturbation ζ . A closer analysis reveals that these two perturbations correspond to two physically distinct modes, the former being a time-delay mode to the big crunch, and the latter a local dilatation in space. In a contracting universe, these two modes are distinct, and they do not mix. It is conceivable that they might mix at the big crunch/big bang transition [35, 36], in which case the scale-invariant contribution would be the dominant one on the large scales of interest, but this possibility is still insufficiently understood to make definite predictions. As we will show next, this is also unnecessary, as there is a very natural *entropic* mechanism which generates scale-invariant curvature perturbations before the big bang, as long as there is more than one scalar field present⁴. But before continuing, it might be useful to add a few remarks concerning the validity of our approach: indeed, the reader might be worried about the validity of perturbation theory, since the background quantities, such as the Hubble rate, as well as the perturbations themselves blow up as $t \rightarrow 0$. However, as shown in [33], after switching to synchronous gauge, it is straightforward to see that the universe evolves to become closer and closer to the unperturbed background solution, and hence perturbation theory is valid. Also, even though the background quantities blow up as seen from the 4-dimensional viewpoint, in fact in the higher-dimensional colliding branes picture the ekpyrotic phase has the effect of flattening the branes and hence of rendering the curvatures *small* as the big crunch is approached [20].

³ Useful asymptotic expressions are $H_\alpha^{(1)}(x) \rightarrow \sqrt{\frac{2}{\pi x}} e^{i(x-\alpha\pi/2-\pi/4)}$ when $x \gg \alpha$ and $H_\alpha^{(1)}(x) \rightarrow -\frac{i}{\pi} \Gamma(\alpha) (\frac{2}{x})^\alpha$ when $x \ll \alpha$ and for $\alpha > 0$.

⁴ Recently, Khoury and Steinhardt have also pointed out that right at the onset of the single-field ekpyrotic phase, a range of scale-invariant modes can be produced [37]. However, contrary to the cases that we have discussed so far, this *adiabatic* mechanism requires the universe to already be contracting when the equation of state is still near $w \approx -1$. If viable, this mechanism would produce an interesting non-gaussian signal; but as it is currently not known how to incorporate this mechanism into a more complete cosmological model, we will not discuss this mechanism here. See also [38] for the challenges that this scenario must address.

B. Two Fields: the Entropic Mechanism

As discussed at the end of the last section, it is rather unnatural to consider only a single scalar field in the effective theory, since there are two universal scalars that are always present in a higher-dimensional context: the radion field, determining the distance between the two end-of-the-world branes, and the volume modulus of the internal manifold. But as soon as there is more than one scalar field present, one can have entropy, or isocurvature, perturbations, which are growing mode perturbations in a collapsing universe [39]. Entropy perturbations can source the curvature perturbation, and hence (provided the entropy perturbations acquire a nearly scale-invariant spectrum), nearly scale-invariant curvature perturbations can be generated just before the bounce [26, 40]. These then turn into growing mode perturbations in the ensuing expanding phase.

For the two scalar fields, we will again assume the potential (21), but with the slight generalization that we allow the fast-roll parameter ϵ to be slowly varying. There are two gauge-invariant scalar perturbation modes: the entropy perturbation $\delta s = \cos \theta \delta \phi_2 - \sin \theta \delta \phi_1$ corresponds to perturbations transverse to the background trajectory, see Fig. 4, while the adiabatic, or curvature, perturbation ζ is the gauge-invariant quantity expressing perturbations along the background trajectory, see [25, 41] for a detailed exposition. For a straight trajectory ($\dot{\theta} = 0$), the linearized equation of motion for δs is

$$\ddot{\delta s} + 3H\dot{\delta s} + \left(\frac{k^2}{a^2} + V_{ss}\right)\delta s = 0, \quad (42)$$

where V_{ss} denotes the second derivative of the potential w.r.t. s . In conformal time, and for the re-scaled variable $\delta S = a(\tau)\delta s$, we obtain

$$\delta S'' + \left(k^2 - \frac{a''}{a} + a^2 V_{ss}\right)\delta S = 0. \quad (43)$$

To proceed, we must relate a''/a and V_{ss} to the fast-roll parameter ϵ and its derivative w.r.t. the number of e-folds of expansion N , where $dN \equiv d \ln a$. By requiring ϵ to vary slowly, what is meant is that we will keep terms in $d\epsilon/dN$, but not higher-order terms such as $d^2\epsilon/dN^2$. Then, by differentiating $\epsilon = \dot{\sigma}^2/(2H^2)$ twice, and using $\ddot{\sigma} + 3H\dot{\sigma} + V_\sigma = 0$ as well as $V_{ss} = V_{\sigma\sigma}$, one can derive the following expressions, valid to sub-leading order in ϵ :

$$\frac{a''}{a} = H^2 a^2 (2 - \epsilon), \quad (44)$$

$$V_{ss} = H^2 \left(-2\epsilon^2 + 6\epsilon + \frac{5}{2}\epsilon_{,N}\right). \quad (45)$$

Using in addition that $aH = (1 + 1/\epsilon + \epsilon_{,N}/\epsilon^2)/(\epsilon\tau)$, Eq. (43) finally reads

$$\delta S'' + \left(k^2 - \frac{2(1 - \frac{3}{2\epsilon} + \frac{3}{4} \frac{\epsilon_{,N}}{\epsilon^2})}{\tau^2} \right) \delta S = 0. \quad (46)$$

In analogy with our discussion of the single-field case, this equation can be solved in terms of the Hankel functions, supplemented by the boundary condition of approaching the Minkowski vacuum state in the far past, to yield (up to a phase)

$$\delta S = \frac{\sqrt{-k\tau}}{2} H_\nu^{(1)}(-k\tau), \quad \nu = \frac{3}{2} \left(1 - \frac{2}{3\epsilon} + \frac{\epsilon_{,N}}{3\epsilon^2} \right). \quad (47)$$

At late times $(-k\tau) \rightarrow 0$ and we obtain

$$\delta S \approx \frac{1}{\sqrt{2}(-\tau)k^\nu}, \quad (48)$$

implying that at the end of the ekpyrotic phase, the entropy perturbation is given by

$$\delta s(t_{ek-end}) \approx \frac{|\epsilon V_{ek-end}|^{1/2}}{\sqrt{2}k^\nu}. \quad (49)$$

Following the same steps as in the single field case above, it is straightforward to see that the spectral index of the entropy perturbation is now given by [26]

$$n_s - 1 = \frac{2}{\epsilon} - \frac{\epsilon_{,N}}{\epsilon^2}. \quad (50)$$

The first term on the right-hand side is a gravitational contribution, which, being positive, tends to make the spectrum blue. The second term is a non-gravitational contribution, which tends to make the spectrum red. A simple way to estimate the natural range of n_s is to rewrite the above expression in terms of \mathcal{N} , the number of e-folds before the end of the ekpyrotic phase (where $d\mathcal{N} = d \ln(aH)$):

$$n_s - 1 = \frac{2}{\epsilon} - \frac{d \ln \epsilon}{d\mathcal{N}}. \quad (51)$$

In this expression, $\epsilon(\mathcal{N})$ measures the equation of state during the ekpyrotic phase, which decreases from a value much greater than unity to a value of order unity in the last \mathcal{N} e-folds. If we estimate $\epsilon \approx \mathcal{N}^\alpha$ [42], then the spectral tilt is

$$n_s - 1 \approx \frac{2}{\mathcal{N}^\alpha} - \frac{\alpha}{\mathcal{N}}. \quad (52)$$

Here we see that the sign of the tilt is sensitive to α . For nearly exponential potentials ($\alpha \approx 1$), the spectral tilt is $n_s \approx 1 + 1/\mathcal{N} \approx 1.02$, slightly blue, because the first term dominates. However, in the cyclic model the steepness of the potential must decrease in order for the ekpyrotic phase to

come to an end, and α parameterizes these cases. If $\alpha > 1.14$, the spectral tilt is red. For example, $n_s = 0.97$ for $\alpha \approx 2$. These examples represent the range that can be achieved by the entropic mechanism, roughly

$$0.97 < n_s < 1.02. \quad (53)$$

These are in good agreement with the present observational bounds obtained by the WMAP satellite, which are $n_s = 0.96 \pm 0.03$ at the 2σ level [9].

Now that we have shown how an approximately scale-invariant spectrum of entropy perturbations may be generated by scalar fields in a contracting universe, we will discuss how these perturbations may be converted to curvature perturbations. Since the entropy perturbations of interest are all of super-horizon scales, we can now restrict our study to large scales only, where spatial gradients can be neglected. On these scales, the evolution equation for the curvature perturbation is given by [25]

$$\dot{\zeta} = -\frac{2H}{\dot{\sigma}}\dot{\theta}\delta s = \sqrt{\frac{2}{\epsilon}}\dot{\theta}\delta s. \quad (54)$$

Hence, as soon as the background trajectory bends ($\dot{\theta} \neq 0$), the entropy perturbations become a source for the curvature perturbations.

There are at least two ways in which such a bending can occur: the first makes use of the instability of the two-field ekpyrotic potential, *cf.* again Fig. 4. If the background trajectory strays sufficiently far from the ridge of the potential, the trajectory will turn and fall off one of the steep sides of the potential [10, 23, 24]. The turning of the trajectory then immediately results in the conversion of entropy into curvature perturbations. Since this conversion occurs during the ekpyrotic phase, we will term this process *ekpyrotic conversion*. It is straightforward to estimate the amplitude of the resulting curvature perturbation (its spectrum will be identical to the spectrum of the entropy perturbations, as Eq. (54) is k -independent): if we approximate the entropy perturbation as remaining constant during the conversion process, and assume a total bending angle of order unity, $\int \dot{\theta} \sim \mathcal{O}(1)$, then the resulting curvature perturbation after conversion will be given by

$$\zeta_{conv-end} \approx \sqrt{\frac{2}{\epsilon_{ek}}}\delta s_{ek-end}. \quad (55)$$

We should mention straight away that the approximations just made will not be good enough in calculating the non-gaussian corrections to the linear calculation, but for the present purposes, they will do. Since the fast-roll parameter $\epsilon_{ek} \sim \mathcal{O}(10^2)$, we find that

$$\zeta_{conv-end} \sim \frac{1}{10}\delta s_{ek-end}. \quad (56)$$

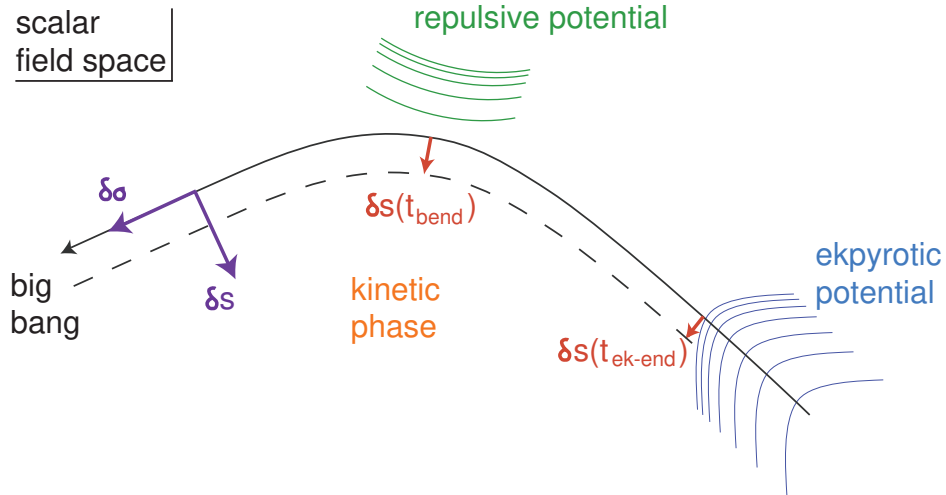


FIG. 5: After the ekpyrotic phase, the trajectory in scalar field space enters the kinetic phase and bends - this bending is described by the existence of an effective repulsive potential (the potentials are indicated by their contour lines). A trajectory adjacent to the background evolution can be characterized by the entropy perturbation $\delta s(t_{ek-end})$ at the end of the ekpyrotic phase, leading to a corresponding off-set $\delta s(t_{bend})$, or equivalently $\delta V(t_{bend})$, at the time of bending.

The second way in which a bending of the trajectory can occur is suggested by the embedding of the cyclic model in M-theory [26], and applies when the background field trajectory remains straight throughout the ekpyrotic phase. At the end of the ekpyrotic phase, the potential turns off, and the evolution becomes dominated by the kinetic energy of the two scalar fields. This kinetic phase corresponds to the final approach of the branes in the higher-dimensional picture. During this approach, there is a generic effect that occurs, but that cannot be seen in the 4-dimensional effective theory. The branes that are bound to collide with each other are of opposite tension. Now, it turns out that just before the collision, it always happens that at the location of the negative tension brane, the internal 6-dimensional manifold tries to shrink to zero size [21]. However, just about any type of matter present on the negative tension brane will smoothly cause the internal manifold to grow again [43]. This effect is due to the special properties of gravity on a negative tension object. When this effect is translated back into the effective theory that we have been using all along, the location in field space where the internal manifold reaches zero size is given by the $\phi_2 = 0$ line. This line thus constitutes a boundary to field space. And the presence of matter on the negative tension brane gives rise to an effective repulsive potential in the vicinity of the $\phi_2 = 0$ line. Hence, during the kinetic phase, the background trajectory automatically bends, just

before the trajectory shoots off to $-\infty$ where the brane collision/big bang occurs. What we have just discussed is a concrete example originating from string theory of how a bend in the trajectory can occur during the kinetic phase. However, more generally our results will apply whatever the microphysical cause of the bending and of the effective repulsive potential, see Fig. 5 for an illustration of the general case that we have in mind. Again, it is quite straightforward to estimate the amplitude of the curvature perturbation resulting from this process of *kinetic conversion*:

On large scales, the linearized equation of motion for the entropy perturbation is given by

$$\ddot{\delta s} + 3H\dot{\delta s} + (V_{ss} + 3\dot{\theta}^2)\delta s = 0, \quad (57)$$

where, incidentally, we have the useful relation $\dot{\theta} = -V_s/\dot{\sigma}$. Then, during the kinetic phase and away from the repulsive potential, the Einstein equations immediately yield

$$H = \frac{1}{3t}, \quad \dot{\sigma} = \frac{-\sqrt{2}}{\sqrt{3}t}. \quad (\text{kinetic phase}) \quad (58)$$

Thus, (57) simplifies to $\ddot{\delta s} + \dot{\delta s}/t = 0$ which implies that the entropy perturbation grows logarithmically during the potential-free kinetic phase. We can ignore this insignificant growth. However, the evolution of the entropy perturbation during the process of conversion turns out to be important. We can estimate it by assuming that the trajectory bends with a constant $\dot{\theta} \sim 1/\Delta t$, where Δt denotes the duration of the conversion process. We can further assume that the repulsive potential depends only on ϕ_2 . Then $\dot{\theta}, V_s, V_{ss}$ can all be related to $V_{,\phi_2}, V_{,\phi_2\phi_2}$, evaluated during the conversion, and it is not difficult to show that this leads to $V_{ss} \approx \dot{\phi}_1\dot{\theta}/(t_{bend}\dot{\phi}_2)$, where t_{bend} corresponds to the time halfway through the bending of the trajectory [44]. For the particular example where the cyclic model is embedded in M-theory, we have that $\dot{\phi}_1 = -\sqrt{3}\dot{\phi}_2$, and specializing to this example, we have $V_{ss} \approx (2-3)\dot{\theta}^2$. Hence, (57) becomes (where we can neglect the term in $\dot{\delta s}$)

$$\ddot{\delta s} + 6\dot{\theta}^2\delta s \approx 0, \quad (59)$$

and thus, during the conversion, the entropy perturbation evolves sinusoidally

$$\delta s \approx \cos[\omega(t - t_{conv-beg})]\delta s(t_{ek-end}), \quad (60)$$

where $t_{conv-beg}$ denotes the time at which the trajectory starts to bend, and $\omega \approx 2.5/\Delta t$. Now we can immediately evaluate the resulting linear curvature perturbation by integrating Eq. (54) to

get

$$\zeta_L = \int_{bend} -\frac{2H}{\dot{\sigma}} \dot{\theta} \delta s \quad (61)$$

$$\approx \sqrt{\frac{2}{3}} \frac{\dot{\theta}}{\omega} \sin(\omega \Delta t) \delta s(t_{ek-end}) \quad (62)$$

$$\approx \frac{1}{5} \delta s(t_{ek-end}). \quad (63)$$

Thus, the amplitude is very similar in magnitude to the value estimated above for the process of ekpyrotic conversion.

We are now in a position to calculate the variance of the generated curvature perturbation, which, on account of (49), is given by

$$\langle \zeta^2 \rangle \approx \int \frac{d^3k}{(2\pi)^3} \frac{\epsilon_{ek} V_{ek-end}}{50k^{2\nu}} = \int \frac{dk}{k} \frac{\epsilon_{ek} V_{ek-end}}{100\pi^2} k^{n_s-1}. \quad (64)$$

Hence, the amplitude is in agreement with the current WMAP bounds of $\Delta_\zeta^2(0.002 Mpc^{-1}) = (2.4 \pm 0.2) \times 10^{-9}$ [9], as long as $|V_{ek-end}| \approx (10^{-2} M_{Pl})^4$, *i.e.* the minimum of the potential has to be roughly at the grand unified scale for models using kinetic conversion [26]. This scale is also the natural scale of Hořava-Witten theory, and thus it is the scale where one would expect the potential to turn around. Note that for models using ekpyrotic conversion, this result implies that the bending must occur at a specific time, namely when the potential reaches the grand unified scale. In the latter models, this may or may not also correspond to the bottom of the potential.

Finally, we should state an important assumption that we have been making implicitly up to now: namely, we assumed that the curvature perturbation passes through the big crunch/big bang transition essentially unchanged. The reason for doing so is that the perturbations we are considering are vastly larger than the horizon size around the time of the crunch, and hence, due to causality, it seems reasonable to assume that long-wavelength modes suffer no change - this viewpoint is discussed in much more detail in [33]. In new ekpyrotic models, in which the bounce is smooth and describable entirely within a 4-dimensional effective theory, this assumption certainly holds true. In the case of a classically singular bounce, this remains an assumption subject to possible revision in the future⁵.

⁵ In this context, we can also mention the possibility that no conversion of entropy to curvature perturbations might occur before the big crunch, but that this conversion could happen during the phase shortly following the bang through modulated reheating [45]: if massive matter fields are produced copiously at the brane collision and dominate the energy density immediately after the bang, and if, furthermore, these fields couple to ordinary matter via a function of δs , then their decay into ordinary matter will occur at slightly different times depending on the value of δs . In this way, the ordinary matter perturbations would also inherit the entropic perturbation spectrum.

IV. HIGHER-ORDER PERTURBATIONS AND PREDICTIONS FOR NON-GAUSSIANITY

A. Definitions and Local Non-Gaussianity

Now that we have seen in detail how the ekpyrotic phase generates linear, nearly scale-invariant density perturbations via the entropic mechanism, we can inquire as to whether the higher-order corrections might lead to an observable signal. We will only calculate non-gaussian corrections for perturbations generated via the entropic mechanism, because, as discussed in the previous section, this is the only robust and well-understood mechanism to date that generates ekpyrotic perturbations in agreement with observations. As we saw earlier, the linear perturbations are related to observations of the 2-point correlation function. Similarly, quadratic and cubic corrections to these perturbations are related to observations of the 3- and 4-point functions respectively. For an exactly gaussian probability distribution, all n -point functions for which n is odd vanish, while for n even, the n -point functions are related to the 2-point function. Thus, the simplest way in which we could detect a departure from exact gaussianity would be due to the presence of a non-vanishing 3-point function.

In momentum space, the 3-point function corresponds to a configuration of 3 momenta, which form a closed triangle due to momentum conservation. Hence, the 3-point function is specified not only by its magnitude on different scales, but also by its magnitude for different shapes of the triangle. Or, turning this reasoning around, when we make predictions for non-gaussianity, we must predict both the amplitude and the shape of the momentum space triangle that we would like to observe. Let us make all of this more precise now. Earlier, we defined the power spectrum as the Fourier transform of the 2-point function,

$$\langle \zeta_{\mathbf{k}_1} \zeta_{\mathbf{k}_2} \rangle = (2\pi)^3 \delta^3(\mathbf{k}_1 + \mathbf{k}_2) P(k_1). \quad (65)$$

Similarly, the *bispectrum*, which is the Fourier transform of the 3-point function, is given by

$$\langle \zeta_{\mathbf{k}_1} \zeta_{\mathbf{k}_2} \zeta_{\mathbf{k}_3} \rangle = (2\pi)^3 \delta^3(\mathbf{k}_1 + \mathbf{k}_2 + \mathbf{k}_3) B(k_1, k_2, k_3), \quad (66)$$

the *trispectrum*, the Fourier transform of the 4-point function, via

$$\langle \zeta_{\mathbf{k}_1} \zeta_{\mathbf{k}_2} \zeta_{\mathbf{k}_3} \zeta_{\mathbf{k}_4} \rangle_c = (2\pi)^3 \delta^3(\mathbf{k}_1 + \mathbf{k}_2 + \mathbf{k}_3 + \mathbf{k}_4) T(k_1, k_2, k_3, k_4), \quad (67)$$

and so on. The δ -functions result from momentum conservation, while B and T are shape functions (for a triangle and a quadrangle respectively). In the last expression, the subscript c indicates that

we only need to consider the connected part of the 4-point function, *i.e.* the part that is not captured by products of 2-point functions.

For non-gaussianity of the so-called *local* form, it is useful to define (in real space) the following expansion of the curvature perturbation on uniform energy density surfaces

$$\zeta = \zeta_L + \frac{3}{5}f_{NL}\zeta_L^2 + \frac{9}{25}g_{NL}\zeta_L^3, \quad (68)$$

with ζ_L being the linear, gaussian part of ζ . The factors of $3/5$ are a historical accident; they arose because this type of expansion was first defined for a different variable. In momentum space, B is then given by

$$B = \frac{6}{5}f_{NL}[P(k_1)P(k_2) + 2 \text{ permutations}], \quad (69)$$

as can be verified straightforwardly by combining Eqs. (65), (66) and (68). Similarly, the momentum space 4-point function corresponding to non-gaussianity of the local form can be expressed as

$$T = \tau_{NL}[P(k_{13})P(k_3)P(k_4) + 11 \text{ perms.}] + \frac{54}{25}g_{NL}[P(k_2)P(k_3)P(k_4) + 3 \text{ perms.}], \quad (70)$$

where τ_{NL} and g_{NL} parameterize the two relevant shape functions, see for example [46] for more details. For cosmological models in which the perturbations originate from the fluctuations of a single field (in our case the entropy field), τ_{NL} is directly related to the square of f_{NL} , explicitly

$$\tau_{NL} = \frac{36}{25}f_{NL}^2. \quad (71)$$

Concentrating now on the bispectrum, we can see that, since for a scale-invariant spectrum $P(k) \sim k^{-3}$, we have

$$B \sim f_{NL}\left(\frac{1}{k_1^3 k_2^3} + \frac{1}{k_2^3 k_3^3} + \frac{1}{k_3^3 k_1^3}\right) \quad (72)$$

$$= f_{NL}\frac{\sum k_i^3}{\prod k_i^3}. \quad (73)$$

This is the typical momentum dependence for local non-gaussianity [47], which is also the relevant one for ekpyrotic models, as we will show shortly. The signal is largest when one of the momenta is very small - this automatically requires the other two momenta to be almost equal, and hence the local form of non-gaussianity corresponds to having the largest signal generated for *squeezed* triangles in momentum space.

It is instructive to calculate explicitly the tree-level 3-point function for the entropy perturbation generated during the ekpyrotic phase, *i.e.* before the conversion to curvature perturbations⁶. Maldacena described in [48] how the expectation value for the 3-point function is given by

$$\langle(\delta s)^3\rangle = -i \int^t dt' \langle[(\delta s)^3(t), H_{int}(t')]\rangle, \quad (74)$$

where $H_{int}(t') = V_{sss}(\delta s)^3/3! = -\sqrt{\epsilon}\kappa_3/(3!t'^2)$ is the cubic interaction Hamiltonian. In Fourier space, this can be rewritten as [12, 49]

$$\begin{aligned} \langle(\delta s)^3\rangle &= (2\pi)^3 \delta(\Sigma_i \mathbf{k}_i) \\ &\times 2\text{Re}\{-i\delta s_{\mathbf{k}_1}(t)\delta s_{\mathbf{k}_2}(t)\delta s_{\mathbf{k}_3}(t) \int_{-\infty}^t \frac{(-\sqrt{\epsilon}\kappa_3)}{t'^2} \delta s_{\mathbf{k}_1}(t')\delta s_{\mathbf{k}_2}(t')\delta s_{\mathbf{k}_3}(t')\}. \end{aligned} \quad (75)$$

For ϵ large, the mode functions are given approximately by (*cf.* Eq. (28))

$$\delta s_{\mathbf{k}}(t) = \frac{1}{\sqrt{2k}} e^{-ikt} \left(1 - \frac{i}{kt}\right), \quad (76)$$

so that we get

$$\langle(\delta s)^3\rangle = (2\pi)^3 \delta(\Sigma_i \mathbf{k}_i) \frac{\sqrt{\epsilon}\kappa_3}{6t^4} \frac{\Sigma k_i^3}{\prod k_i^3}, \quad (77)$$

where we have used the result that

$$\begin{aligned} &i(1 + ik_1 t)(1 + ik_2 t)(1 + ik_3 t) e^{-iKt} \int (1 - ik_1 t')(1 - ik_2 t')(1 - ik_3 t') e^{iKt'} (t')^{-5} + c.c. \\ &= \frac{1}{2} \Sigma_i k_i^3 + \dots, \end{aligned} \quad (78)$$

with $K = k_1 + k_2 + k_3$ and where the dots indicate terms suppressed by powers of $k_i t$. The calculation shows two things: first, the momentum dependence in (77) is of the local form, and, comparing with (69) and using $P_{\delta s}(k) = 1/(2t^2 k^3)$ from (31) and (34), it corresponds to having an entropy perturbation of the form

$$\delta s = \delta s_L + \frac{\sqrt{\epsilon}\kappa_3}{8} \delta s_L^2, \quad (79)$$

where δs_L is the linear, gaussian part of the entropy perturbation δs . Secondly, the end-result is dominated by the terms for which $|k_i t| \ll 1$ - in other words, the dominant contribution to non-gaussianity is generated by the (classical) evolution on super-horizon scales, and the same holds true for the 4-point function also. Hence, in determining the predictions for the non-gaussian curvature

⁶ Note that quantum corrections from loop diagrams will be suppressed by factors of \hbar .

perturbation, we can simply perform the calculation using the higher-order classical equations of motion on large scales, up to the required order in perturbation theory.

The strategy for calculating the non-linearity parameters defined in (68) is straightforward: first we solve the equation of motion for the entropy perturbation up to third order in perturbation theory. This allows us to integrate the equation of motion for ζ , at the first three orders in perturbation theory, and then we obtain the non-linearity parameters by evaluating

$$f_{NL} = \frac{5}{3} \frac{\int_{t_{ek-beg}}^{t_{conv-end}} \zeta^{(2)'}}{(\int_{t_{ek-beg}}^{t_{conv-end}} \zeta^{(1)'})^2}, \quad g_{NL} = \frac{25}{9} \frac{\int_{t_{ek-beg}}^{t_{conv-end}} \zeta^{(3)'}}{(\int_{t_{ek-beg}}^{t_{conv-end}} \zeta^{(1)'})^3}, \quad (80)$$

where the integrals are evaluated from the time that the ekpyrotic phase begins until the conversion phase has ended and ζ has evolved to a constant value. A note on notation: we expand the entropy perturbation (and similarly the curvature perturbation) as

$$\delta s = \delta s^{(1)} + \delta s^{(2)} + \delta s^{(3)} \quad (81)$$

without factorial factors and where we use $\delta s^{(1)}$ and δs_L interchangeably (in section III, where we dealt exclusively with linear perturbations, we sometimes wrote δs instead of $\delta s^{(1)}$, but hopefully this will not confuse the reader).

The relevant equations of third order cosmological perturbation theory with multiple scalar fields was developed in [50], and we will use the results of that paper. The derivations of the equations are lengthy, and do not provide any further insight into the topic of this review. Hence, we will simply use the equations as we need them. Interestingly, it turns out that all results regarding the conversion process can be well approximated by various simple techniques that we will present further below, both for ekpyrotic and for kinetic conversion.

B. Generation of Entropy Perturbations

During the ekpyrotic phase, the equation of motion for the entropy perturbation, up to third order in perturbation theory, is given by [50]

$$\begin{aligned} & \ddot{\delta s} + 3H\dot{\delta s} + V_{,ss}\delta s + \frac{1}{2}V_{,sss}(\delta s)^2 \\ & + \frac{V_{,\sigma\sigma}}{\dot{\sigma}^3}(\dot{\delta s})^3 + \left(\frac{V_{,\sigma\sigma}}{\dot{\sigma}^2} + 3\frac{V_{,\sigma}^2}{\dot{\sigma}^4} + 3H\frac{V_{,\sigma}}{\dot{\sigma}^3} - 2\frac{V_{,ss}}{\dot{\sigma}^2} \right) (\dot{\delta s})^2\delta s \\ & + \left(-\frac{3}{2\dot{\sigma}}V_{,s\sigma\sigma} - 5\frac{V_{,\sigma}V_{,ss}}{\dot{\sigma}^3} - 3H\frac{V_{,ss}}{\dot{\sigma}^2} \right) \dot{\delta s}(\delta s)^2 + \left(\frac{1}{6}V_{,ssss} + 2\frac{V_{,\sigma}^2}{\dot{\sigma}^2} \right) (\delta s)^3 = 0. \end{aligned} \quad (82)$$

Using the following expressions, valid during the ekpyrotic phase,

$$\begin{aligned} \dot{\sigma} &= -\frac{\sqrt{2}}{\sqrt{\epsilon t}} & V &= -\frac{1}{\epsilon t^2} \\ V_{,\sigma} &= -\frac{\sqrt{2}}{\sqrt{\epsilon t^2}} & V_{,\sigma\sigma} &= -\frac{2}{t^2} & V_{,s\sigma} &= 0 & V_{,ss\sigma} &= -\frac{2\sqrt{2}\epsilon}{t^2} \\ V_{,s} &= 0 & V_{,ss} &= -\frac{2}{t^2} & V_{,sss} &= -\frac{\kappa_3\sqrt{\epsilon}}{t^2} & V_{,ssss} &= -\frac{\kappa_4\epsilon}{t^2}, \end{aligned}$$

it is not difficult to find by iteration that the entropy perturbation, to leading order in $1/\epsilon$, is given by

$$\delta s = \delta s_L + \frac{\kappa_3\sqrt{\epsilon}}{8}\delta s_L^2 + \epsilon\left(\frac{\kappa_4}{60} + \frac{\kappa_3^2}{80} - \frac{2}{5}\right)\delta s_L^3, \quad (83)$$

where, just as before, $\delta s_L \propto 1/t$. Note that the quadratic term agrees exactly with (79). At each order in perturbation theory, the non-linear corrections depend on the parameters of the potential at that order, *cf.* the parametrization of the potential in Eq. (21). The above equation specifies the initial conditions for the start of the conversion phase.

Both during the ekpyrotic phase and during the conversion process, when the background trajectory bends, the entropy perturbation sources the curvature perturbation on large scales according to [50]

$$\begin{aligned} \dot{\zeta} &\approx \frac{2H}{\dot{\sigma}^2} [V_{,s}\delta s - \frac{1}{2\dot{\sigma}}V_{,\sigma}\delta s\dot{\delta s} + (\frac{1}{2}V_{,ss} + \frac{2}{\dot{\sigma}^2}V_{,s}^2)(\delta s)^2] \\ &+ \frac{2H}{\dot{\sigma}^2} [(-\frac{\dot{\theta}}{6\dot{\sigma}^2}V_{,\sigma} - \frac{1}{2\dot{\sigma}}V_{,s\sigma} - \frac{2}{\dot{\sigma}^3}V_{,s}V_{,\sigma})(\delta s)^2\dot{\delta s} + (\frac{1}{6}V_{,sss} + \frac{2}{\dot{\sigma}^2}V_{,s}V_{,ss} + \frac{4}{\dot{\sigma}^4}V_{,s}^3)(\delta s)^3]. \quad (84) \end{aligned}$$

The inelegant, but sure-fire thing to do now is to simply integrate this equation numerically during the two phases of generation and conversion, and to deduce the non-linearity parameters using (80), as was done in [50]. However, this approach does not give much insight into the final result. This is why we will present more physically transparent techniques first, which allow us to estimate the non-linearity parameters f_{NL} and g_{NL} pretty well, and subsequently we will compare these estimates with the results of numerical integration and discuss the predictions.

C. Ekpyrotic Conversion

We start by analyzing the case where the conversion of entropy into curvature modes occurs during the ekpyrotic phase. For this scenario, it was shown by Koyama *et al.* [49] that the so-called δN formalism [51, 52] is well suited. For ekpyrotic conversion, the calculation is most easily performed, and the result most easily expressed, in terms of the potential (18), which is why we are

adopting this restricted form here. In working with a parameterized potential like (21), the bending of the trajectory can be more complicated, in the sense that there can be multiple turns, and one has to decide when to stop the evolution. In this case, the results are strongly cut-off dependent, and without a precisely defined model specifying the subsequent evolution, it is impossible to make any generic predictions.

The δN formalism is particularly well suited to the case of ekpyrotic conversion, because the background evolution is simple. In fact, it turns out that by making the approximation that the bending is instantaneous, it is very easy to find an approximate formula for the non-linearity parameters at any chosen order in perturbation theory. The following calculation was first presented in [49] for the bispectrum, and trivially extended to the trispectrum in [50].

In order to implement the δN formalism, we have to calculate the integrated expansion $N = \int H dt$ along the background trajectory. Initially, the trajectory is close to the scaling solution (22). Then, we assume that at a fixed field value δs_B away from the ridge, the trajectory instantly bends and rolls off along the ϕ_2 direction. At this point, the trajectory follows the single-field evolution

$$a(t) = (-t)^{2/c_2^2} \quad \phi_2 = \frac{2}{c_2} \ln(-t) + \text{constant} \quad \phi_1 = \text{constant}. \quad (85)$$

Approximating the bending as instantaneous, it is easy to evaluate the integrated expansion, with the result that

$$N = -\frac{2}{c_1^2} \ln |H_B| + \text{constant}, \quad (86)$$

where H_B denotes the Hubble parameter at the instant that the bending occurs. Note that all c_2 -dependence has canceled out of the formula above. At the end of the conversion process, we are interested in evaluating the curvature perturbation on a surface of constant energy density. But, on a surface of constant energy density, the curvature perturbation is equal to a perturbation in the integrated expansion [53]. If we assume that the integrated expansion depends on a single variable α , we can write

$$\zeta = \delta N = N_{,\alpha} \delta\alpha + \frac{1}{2} N_{,\alpha\alpha} (\delta\alpha)^2 + \frac{1}{6} N_{,\alpha\alpha\alpha} (\delta\alpha)^3. \quad (87)$$

In our example, we indeed expect a change in N to depend solely on a change in the initial value of the entropy perturbation δs . Now, from Eq. (83), we know that $\delta s_L \propto 1/t \propto H$, and hence we can parameterize different initial values of the entropy perturbation by writing

$$\delta s_L = \alpha H. \quad (88)$$

Note that since δs_L is gaussian, so is α . With this identification, we have

$$\delta s = \alpha H + \frac{\kappa_3 \sqrt{\epsilon}}{8} (\alpha H)^2 + \epsilon \left(\frac{\kappa_4}{60} + \frac{\kappa_3^2}{80} - \frac{2}{5} \right) (\alpha H)^3, \quad (89)$$

so that at the fixed value $\delta s = \delta s_B$, we have

$$\alpha \propto \frac{1}{H_B}. \quad (90)$$

Now we can immediately evaluate

$$N_{,\alpha} = N_{,H_B} \frac{dH_B}{d\alpha} = \frac{2}{c_1^2 \alpha}, \quad (91)$$

and similarly

$$N_{,\alpha\alpha} = -\frac{2}{c_1^2 \alpha^2} \quad N_{,\alpha\alpha\alpha} = \frac{4}{c_1^2 \alpha^3}. \quad (92)$$

In this way, with very little work, we can estimate the non-linearity parameters

$$f_{NL} = \frac{5N_{,\alpha\alpha}}{6N_{,\alpha}^2} = -\frac{5}{12} c_1^2 \quad (93)$$

$$\tau_{NL} = \frac{36}{25} f_{NL}^2 = \frac{1}{4} c_1^4 \quad (94)$$

$$g_{NL} = \frac{25N_{,\alpha\alpha\alpha}}{54N_{,\alpha}^3} = \frac{25}{108} c_1^4. \quad (95)$$

We are now in a position to compare these estimates to the numerical results obtained in [50] by solving and integrating the equations of motion (82) and (84)⁷. There, the initial conditions were chosen such that they are given by the scaling solution (22), except for an 0.1 percent increase in the initial field velocity $|\dot{\phi}_2|$. This causes the trajectory to eventually roll off in the ϕ_2 direction, and to quickly approach the single-field solution (85). The results for several values of c_1 and c_2 are shown table I, alongside the values estimated by the δN formulae.

It is immediately apparent that the general trend is accurately captured by the δN formulae. However, one may notice that the agreement is slightly less good at third order than at second, and also, that the δN formulae tend to slightly over-estimate τ_{NL} and slightly under-estimate g_{NL} . But given the quickness of the δN calculation and the complexity of the third order equations of motion, the agreement is pretty impressive. Of course, the δN formula was derived subject to the instantaneous bending approximation. Without this approximation, we would expect a numerical scheme that uses the δN formalism to yield results in close agreement with the numerical results.

⁷ Approximate analytic solutions to the equations of motion were first presented in [54].

c_1	c_2	$f_{NL,\delta N}$	$\tau_{NL,\delta N}$	$g_{NL,\delta N}$	f_{NL}	τ_{NL}	g_{NL}
10	10	-41.67	2500	2315	-39.95	2298	2591
10	15	-41.67	2500	2315	-40.45	2356	2813
10	20	-41.67	2500	2315	-40.62	2377	3030
15	10	-93.75	12660	11720	-91.01	11930	13100
15	15	-93.75	12660	11720	-92.11	12220	13830
15	20	-93.75	12660	11720	-92.49	12320	14440
20	10	-166.7	40000	37040	-162.5	38020	41320
20	15	-166.7	40000	37040	-164.4	38930	43170
20	20	-166.7	40000	37040	-165.1	39240	44490

TABLE I: Ekpyrotic conversion: the values of the non-linearity parameters estimated by the δN formalism (using the instantaneous bending approximation) compared to the numerical results obtained by directly integrating the equations of motion, for potentials of the form $V = -V_1 e^{-c_1 \phi_1} - V_2 e^{-c_2 \phi_2}$.

D. Kinetic Conversion

As discussed in more detail at the end of section III, in models motivated by M-theory a bend in the trajectory happens naturally just before the big crunch, during the final approach of the two end-of-the-world branes. This bend takes place after the ekpyrotic phase has come to an end and while the evolution of the universe is dominated by the kinetic energies of the scalar fields - see also Fig. 5. Again, there exists a simple approach to estimate the non-gaussianity parameters of the curvature perturbation generated by this process of kinetic conversion, and we will review it here. This simplified approach was first presented in [55], based on previous work in [44, 50, 54, 56].

This estimating procedure is based on the fact that the physics of the kinetic phase is really quite simple, and moreover, except for the fact that its initial conditions involve the entropy perturbation δs , the kinetic phase has no memory of the details of the ekpyrotic phase. In particular, only the total δs in (83) matters, and the way we choose to decompose it into linear, second- and third-order parts is irrelevant at this point. What is more, since $\delta s_L \ll 1$, the second and third order terms in (83) are highly subdominant and we can approximate the evolution of δs by that of the linear term δs_L throughout the kinetic phase. This realization is the first ingredient of the calculation.

The second is a compact and very useful expression for the evolution of the curvature perturbation ζ on large scales and on surfaces of constant energy density [53, 54]:

$$\dot{\zeta} = \frac{2\bar{H}\delta V}{\dot{\sigma}^2 - 2\delta V}, \quad (96)$$

where $\delta V \equiv V(t, x^i) - \bar{V}(t)$ and a bar denotes a background quantity. This equation is exact in the

limit where spatial gradients can be neglected, and can thus be expanded up to the desired order in perturbation theory if required. If expanded, it corresponds precisely to Eq. (84) [55].

The third and last ingredient of the calculation is the simple relationship between δV and δs during the conversion process. As we saw earlier, during the ekpyrotic phase, the curvature perturbation picks up a blue spectrum and is hence completely negligible on large scales. To be precise, since $\delta V \neq 0$ during ekpyrosis, there is already some conversion of entropy into curvature perturbations occurring at this stage. However, this contribution is entirely negligible compared to the subsequent conversion (note that since $V_{,s} = 0$ during ekpyrosis, δV starts out at subleading order), and hence we can take $\zeta(t_{ek-end}) \approx 0$. Moreover, as we saw when we were discussing the linear perturbations, at the end of the conversion process ζ is still significantly smaller than δs , being given by

$$\zeta_L \approx \frac{1}{5} \delta s_L. \quad (97)$$

Hence, during the conversion process, we can take the potential to depend only on δs . And since the repulsive potential is monotonic and we are interested in small departures $\delta s \ll 1$ from the background trajectory, it is intuitively clear that δV is directly proportional to δs during the bending. A numerical calculation readily confirms this simple relationship.⁸

During the conversion, the effect of the repulsive potential is to cause the entropy perturbation to behave approximately sinusoidally, as shown in Eq. (60). As we will confirm below, during the conversion process $\delta V \ll \dot{\sigma}^2$, so that Eq. (96) simplifies further to

$$\dot{\zeta} \approx \frac{2\bar{H}}{\dot{\sigma}^2} \delta V, \quad (98)$$

which, when integrated and upon use of (58) immediately reproduces Eq. (97). But, as argued above, δs as a whole must behave approximately in this way during the conversion phase, and subsequently analogous relationships must hold at higher orders too:

$$\zeta^{(2)} \approx \frac{1}{5} \frac{\kappa_3 \sqrt{\epsilon}}{8} \delta s_L^2, \quad \zeta^{(3)} \approx \frac{1}{5} \left(\frac{\kappa_4}{60} + \frac{\kappa_3^2}{80} - \frac{2}{5} \right) \epsilon \delta s_L^3. \quad (99)$$

These expressions immediately allow us to calculate the non-linearity parameters

$$f_{NL} \equiv \frac{5}{3} \frac{\zeta^{(2)}}{\zeta_L^2} \approx 3\kappa_3 \sqrt{\epsilon}, \quad (100)$$

$$g_{NL} \equiv \frac{25}{9} \frac{\zeta^{(3)}}{\zeta_L^3} \approx 70 \left(\frac{\kappa_4}{60} + \frac{\kappa_3^2}{80} - \frac{2}{5} \right) \epsilon. \quad (101)$$

⁸ For completeness, we mention that the curvature perturbation can also be sourced by perturbations in the comoving energy density [41]. However, the ekpyrotic phase massively suppresses comoving energy density perturbations on large scales; since the kinetic phase is relatively short, they do not have time to grow and become significant, so that we can neglect them in our calculation - see also [56].

Thus, without much work at all, we find these simple estimates for the non-linearity parameters.

Before discussing this result, let us briefly pause to verify the approximation made in obtaining Eq. (98): during the kinetic phase, we can rewrite (96) as

$$\dot{\zeta} = \frac{t \delta V}{1 - 3t^2 \delta V}. \quad (102)$$

The approximation made above consists in writing $\dot{\zeta} \approx t \delta V$ and this leads to $\zeta \approx \frac{1}{2} t_{\text{bend}}^2 \delta V(t_{\text{bend}})$. But we know that by the end of the conversion process $\zeta \approx \frac{1}{5} \delta s$ and hence we find that

$$3t_{\text{bend}}^2 \delta V \approx \delta s \ll 1, \quad (103)$$

which shows that the approximation is self-consistent and confirms the validity of (98).

The results above indicate that the non-linearity that was present in the entropy perturbation gets transferred straightforwardly (*i.e.* only with an overall numerical coefficient) to the non-linearity in the curvature perturbation, essentially due to the simplicity of the kinetic phase. This calculation therefore leads us to expect no significant additional constant terms in f_{NL} or constants and κ_3 -dependent terms in g_{NL} ; we will see shortly that this expectation is indeed borne out.

We can now compare these estimates to the results of brute-force numerical integration [50]. As discussed in section III, the repulsive potential can in principle be calculated, given a specific matter configuration on the negative-tension brane [43]. Here, we consider four different examples for the repulsive potential

$$V_{\text{rep}} \propto \phi_2^{-2}, \phi_2^{-2} + \phi_2^{-6}, (\sinh \phi_2)^{-2}, (\sinh \phi_2)^{-2} + (\sinh \phi_2)^{-4}, \quad (104)$$

with the overall magnitude adjusted in order to obtain various values for the duration of the conversion (see below). These potential forms should give an indication of the range of values that one can expect the non-linearity parameters to take. Note that, without loss of generality, we take the boundary to be located at $\phi_2 = 0$, and we only consider conversions during which $\dot{\theta} > 0$ – other cases can be related to these by an appropriate change of coordinates.

An important parameter turns out to be the duration of the conversion [50, 56], measured by the number of Hubble times during which most, say 90 percent, of the conversion takes place, *i.e.* the duration is measured by the number of e-folds by which the scale factor shrinks during conversion. Conversions lasting less than about 0.2 Hubble times correspond to what we call sharp conversions, while those that last on the order of 1 Hubble time correspond to smooth conversions. It turns out that the estimating procedure presented above works best for the case of smooth conversions. For f_{NL} , the range of predicted values is considerably narrower as the conversion becomes smoother

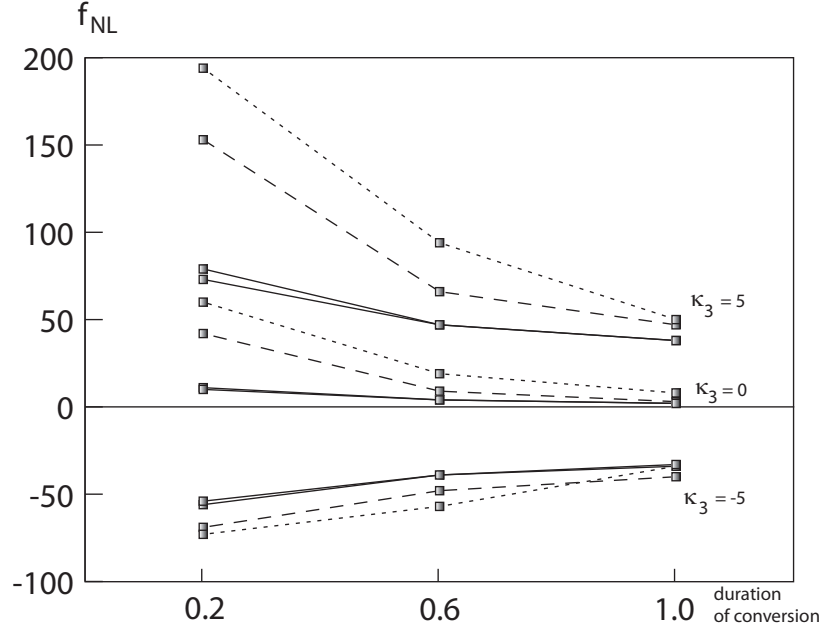


FIG. 6: f_{NL} as a function of the duration of conversion and for the values $\kappa_3 = -5, 0, 5$ and $\epsilon = 36$. In each case, we have plotted the results for four different reflection potentials, with the simplest potentials $(\phi_2^{-2}, (\sinh \phi_2)^{-2})$ indicated by solid lines, while the dashed $((\sinh \phi_2)^{-2} + (\sinh \phi_2)^{-4})$ and dotted $(\phi_2^{-2} + \phi_2^{-6})$ lines give an indication of the range of values that can be expected. As the conversions become smoother, the predicted range of values narrows, and smooth conversions lead to a natural range of about $-50 \lesssim f_{NL} \lesssim +60$ or so.

[44, 56], as illustrated in Fig. 6. Moreover, f_{NL} can be well fitted by

$$f_{NL} = \frac{3}{2} \kappa_3 \sqrt{\epsilon} + 5, \quad (105)$$

in good agreement with the simple estimate (100).

We will show the results for g_{NL} slightly more explicitly; they are illustrated in Figs. 7 and 8. In each case, we have plotted the results obtained for the four repulsive potentials (104). The left panel of Fig. 7 shows that, even more so than for f_{NL} , the range of predicted values for g_{NL} narrows drastically as the conversion process becomes smoother. In fact, for sharp conversions, typical values are very large in magnitude, and we expect these to be observationally disfavored shortly, if they are not ruled out already. Thus, phenomenologically speaking, it is much more interesting to focus on smooth conversions. The right panel in Fig. 7 shows that g_{NL} is proportional to ϵ , while Fig. 8 indicates that g_{NL} depends linearly on κ_4 and approximately quadratically on κ_3 . In fact, all numerical results indicate that g_{NL} scales with $\epsilon, \kappa_3, \kappa_4$ exactly as the third-order coefficient in the expression (83) for the entropy perturbation during the ekpyrotic phase, and the data can be

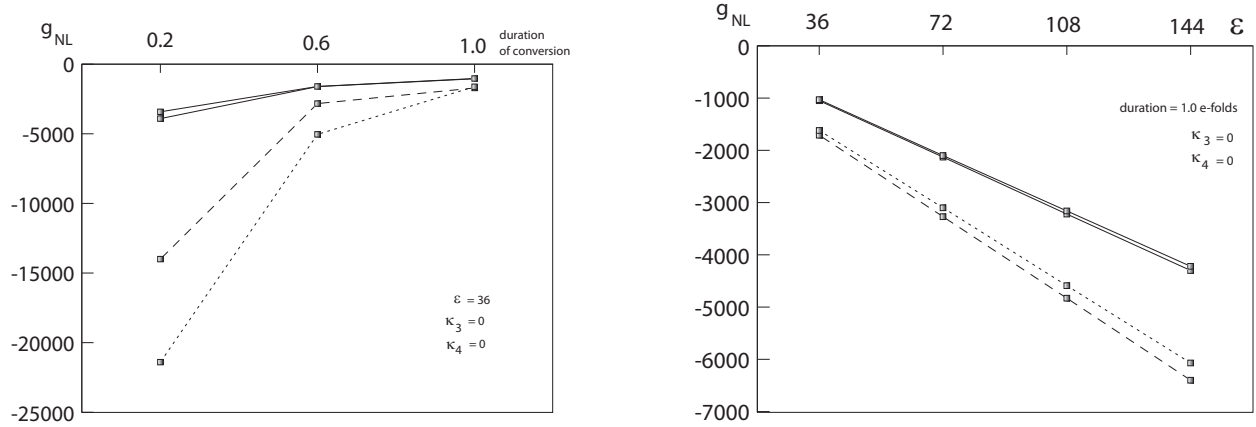


FIG. 7: On the left, g_{NL} is shown as a function of the duration of conversion, with $\kappa_3 = \kappa_4 = 0$ and for four different reflection potentials, and with the same line style assignments as in Fig. 6. As the conversions become smoother, the predicted range of values narrows considerably, allowing rather definite predictions. On the right, g_{NL} can be seen to be proportional to ϵ , *i.e.* proportional to the equation of state w_{ek} .

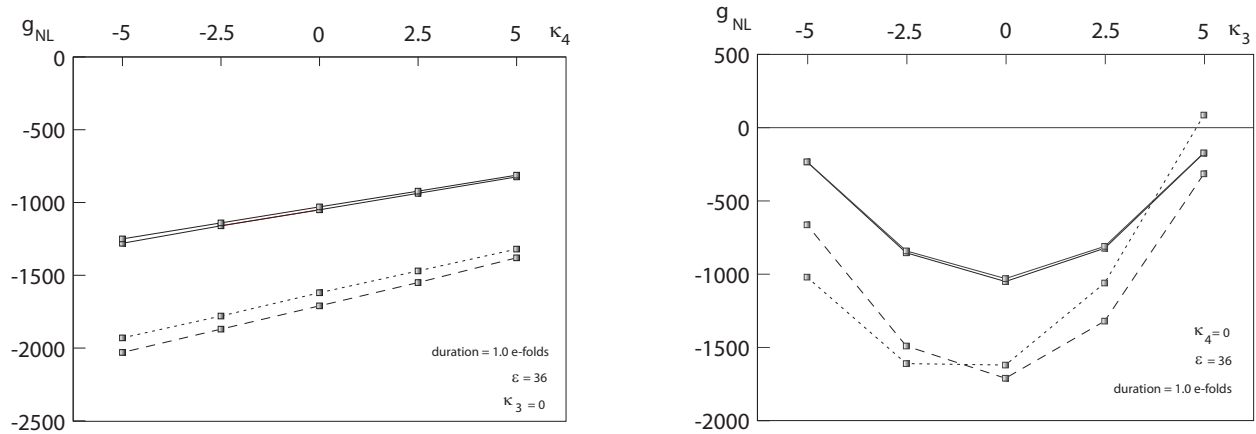


FIG. 8: The left figure indicates that g_{NL} depends linearly in κ_4 , the parameter we are using to specify the fourth derivative of the ekpyrotic potential with respect to the entropic direction. Similarly, in the right figure g_{NL} can be seen to depend approximately quadratically on κ_3 , the parameter determining the third derivative of the ekpyrotic potential with respect to the entropic direction.

fitted by the approximate formula

$$g_{NL} \approx 100 \left(\frac{\kappa_4}{60} + \frac{\kappa_3^2}{80} - \frac{2}{5} \right) \epsilon, \quad (106)$$

again in good agreement with the estimate (101).

V. DISCUSSION OF THE RESULTS

In this review, we have focussed on the predictions for non-gaussianity generated via the entropic mechanism in ekpyrotic models and their cyclic extensions. The reason for concentrating on the entropic mechanism is that this is currently the most robust, best-motivated and best-understood mechanism for generating nearly scale-invariant curvature perturbations during a contracting phase of the universe. As indicated by its name, the entropic mechanism achieves this by first generating nearly scale-invariant entropy perturbations, which are subsequently converted into curvature perturbations. There are essentially two distinct possibilities for when this conversion can happen: either directly during the ekpyrotic phase (*ekpyrotic conversion*) or during the subsequent phase of scalar field kinetic energy domination right before the big crunch/big bang transition (*kinetic conversion*). In both cases, the curvature perturbations pick up non-gaussian corrections of the local form, although the magnitude of the second and third order non-linearity parameters f_{NL} and g_{NL} differ substantially for the two modes of conversion. For convenience, we will repeat the predictions here:⁹

$$f_{NL} = -\frac{5}{12}c_1^2 \quad \text{Ekpyrotic Conversion} \quad (107)$$

$$g_{NL} = \frac{25}{108}c_1^4, \quad (108)$$

$$f_{NL} = \frac{3}{2}\kappa_3 \sqrt{\epsilon} + 5 \quad \text{Kinetic Conversion} \quad (109)$$

$$g_{NL} = \left(\frac{5}{3}\kappa_4 + \frac{5}{4}\kappa_3^2 - 40\right)\epsilon. \quad (110)$$

For ekpyrotic conversion, the results are presented in terms of the parameters of the ekpyrotic potential as expressed in (18). The first thing to note is that the signs are unambiguously fixed: f_{NL} is predicted to be always negative, while g_{NL} is always positive. In order for the power spectrum of the perturbations to be in agreement with observations, one needs $c_1 \gtrsim 10$, which implies $f_{NL} \lesssim -40$ and $g_{NL} \gtrsim 2500$. The current observational bounds are that $f_{NL} = 38 \pm 21$, where the errors are quoted at 1σ [57], while currently no strong constraints exist yet on g_{NL} . These values put the predicted values for f_{NL} for ekpyrotic conversion at 4σ or more from the

⁹ We should caution the reader that what we are presenting here are the predictions from the ekpyrotic phase alone, *i.e.* we have assumed that the primordial density perturbations generated by the ekpyrotic phase have not been modified by the dynamics of the big crunch/big bang transition, nor that there are additional effects of relevance during the first stages of the subsequent expanding phase of the universe (it is conceivable, for example, that models might be constructed which utilize the ekpyrotic phase, but where there are additional fields that are relevant during the expanding phase and which would contribute to the curvature perturbation - in this case, the final predictions will evidently be model-dependent).

central value, and thus this type of conversion is on the verge of being ruled out by observations. What this means for model-building is that models that have made use of the ekpyrotic conversion mechanism, such as new ekpyrotic models [10, 12], might have to be modified in a way such that the conversion occurs only once the equation of state becomes small. This is not unnatural, as the ekpyrotic phase must come to an end anyhow before the bounce phase begins, and if the conversion occurs after the end of the ekpyrotic phase, the predictions will be closer to those predicted by the kinetic conversion mechanism, which we turn our attention to now.

For kinetic conversion, the results (109) and (110) are presented in terms of the parameters of the ekpyrotic potential as written in (21). The parameters κ_3, κ_4 are expected to be of $\mathcal{O}(1)$. The fast-roll parameter ϵ is typically of $\mathcal{O}(10^2)$, with a lower bound of about 50 in order for the power spectrum to be in agreement with observations. Thus, the fitting formulae predict the bispectrum parameter f_{NL} to be of order a few tens, with the sign being typically determined by the sign of κ_3 . This is in good agreement with current bounds for very natural values of the parameters, such as $\epsilon = 100$ and $-1 \lesssim \kappa_3 \lesssim 5$, for example. The associated prediction for the trispectrum g_{NL} is rather interesting, owing to the fact that the κ_3, κ_4 -independent contribution is quite large. It sets the “central” value of the prediction at -40ϵ and thus tends to make g_{NL} of order a few thousand and *negative* in sign. Even with largish values of $\kappa_3 \sim 5$ and $\kappa_4 \sim 5$, the prediction is still negative $g_{NL} \sim -\epsilon$, and hence the negative sign of g_{NL} is a rather robust prediction of the kinetic conversion mechanism. For completeness, we note that the second trispectrum parameter τ_{NL} is always given in terms of f_{NL} according to (71), and thus it is predicted to be positive and of order a few hundred. Observational limits on τ_{NL} will thus provide a consistency check of the predictions, and will give an indication whether or not the fluctuations of a single field (in this case the entropy field) were at the origin of the final spectrum of curvature perturbations.

What are the implications of these predictions? Assuming that the observational error bars quoted above will shrink in the near future and that the ekpyrotic conversion mechanism will be ruled out, we will focus here on the predictions of the kinetic conversion mechanism. The most interesting feature is that the natural ranges of the non-linearity parameters are at a level that will be observable by near-future experiments, perhaps already with the PLANCK satellite. Hence, in a few years, we will know whether or not ekpyrotic models, in combination with the entropic mechanism, will be viable or even preferred by the data. In this vein, it is useful to briefly contrast the predictions discussed here with those of inflationary models¹⁰: for simple, single-field

¹⁰ Here, we only contrast the predictions for non-gaussianity of the local form. Non-canonical kinetic terms addition-

inflationary models the predicted values for all non-linearity parameters are very small, of order 1 or smaller [48, 59]. Even though these values lie within the predicted ranges of the kinetic conversion mechanism, it is clear that, since these values arise naturally for single-field inflationary models whereas obtaining the same small values in ekpyrosis would require a very finely tuned potential, in case of a non-detection of non-gaussianity the simple inflationary models will be strongly preferred. Conversely, since multi-field inflationary models can give rise to just about any values of the non-linearity parameters [60], in case of a detection of non-gaussianity compatible with the values predicted by the kinetic conversion mechanism, those latter models will be preferred by the data. At that point it will be necessary to include also the observational evidence for or against primordial scale-invariant gravitational waves. Such gravity waves would strongly favor inflationary models, whereas their absence is compatible with ekpyrotic models. The absence of primordial scale-invariant gravitational waves, combined with local non-gaussianity parameters in the ranges predicted by (109) and (110), would be nothing short of spectacular, as they would point towards the existence of a contracting phase prior to the big bang, and open up the possibility of a multiverse in time, with correspondingly vast timescales unlike anything we are used to in cosmology right now.

Acknowledgments

I would like to thank Sébastien Renaux-Petel and Paul Steinhardt for very enjoyable collaborations on the subject of this review. I would also like to thank Justin Khoury, Kazuya Koyama, Burt Ovrut, Neil Turok and David Wands for stimulating and informative discussions.

-
- [1] D. Baumann (2009), 0907.5424.
 - [2] R. Brustein and P. J. Steinhardt, Phys. Lett. **B302**, 196 (1993), hep-th/9212049.
 - [3] A. Borde, A. H. Guth, and A. Vilenkin, Phys. Rev. Lett. **90**, 151301 (2003), gr-qc/0110012.
 - [4] A. H. Guth, J. Phys. **A40**, 6811 (2007), hep-th/0702178.
 - [5] J.-L. Lehners, Phys. Rept. **465**, 223 (2008), 0806.1245.
 - [6] D. Seery and J. E. Lidsey, JCAP **0509**, 011 (2005), astro-ph/0506056.

ally generate non-gaussianities with different shapes in momentum space, such as equilateral triangles in the case of the bispectrum. This is well understood for inflation, but has not been much explored yet for ekpyrotic models - though see [58] for a related study.

- [7] J. Khoury, B. A. Ovrut, P. J. Steinhardt, and N. Turok, Phys. Rev. **D64**, 123522 (2001), hep-th/0103239.
- [8] J. K. Erickson, S. Gratton, P. J. Steinhardt, and N. Turok, Phys. Rev. **D75**, 123507 (2007), hep-th/0607164.
- [9] E. Komatsu et al. (WMAP), Astrophys. J. Suppl. **180**, 330 (2009), 0803.0547.
- [10] E. I. Buchbinder, J. Khoury, and B. A. Ovrut, Phys. Rev. **D76**, 123503 (2007), hep-th/0702154.
- [11] E. I. Buchbinder, J. Khoury, and B. A. Ovrut, JHEP **11**, 076 (2007), arXiv:0706.3903 [hep-th].
- [12] P. Creminelli and L. Senatore, JCAP **0711**, 010 (2007), hep-th/0702165.
- [13] N. Arkani-Hamed, H.-C. Cheng, M. A. Luty, and S. Mukohyama, JHEP **05**, 074 (2004), hep-th/0312099.
- [14] A. Adams, N. Arkani-Hamed, S. Dubovsky, A. Nicolis, and R. Rattazzi, JHEP **10**, 014 (2006), hep-th/0602178.
- [15] R. Kallosh, J. U. Kang, A. D. Linde, and V. Mukhanov, JCAP **0804**, 018 (2008), 0712.2040.
- [16] P. J. Steinhardt and N. Turok (2001), hep-th/0111030.
- [17] P. J. Steinhardt and N. Turok, Phys. Rev. **D65**, 126003 (2002), hep-th/0111098.
- [18] A. Lukas, B. A. Ovrut, K. S. Stelle, and D. Waldram, Phys. Rev. **D59**, 086001 (1999), hep-th/9803235.
- [19] P. Horava and E. Witten, Nucl. Phys. **B460**, 506 (1996), hep-th/9510209.
- [20] N. Turok, M. Perry, and P. J. Steinhardt, Phys. Rev. **D70**, 106004 (2004), hep-th/0408083.
- [21] J.-L. Lehners, P. McFadden, and N. Turok, Phys. Rev. **D75**, 103510 (2007), hep-th/0611259.
- [22] J.-L. Lehners, P. McFadden, and N. Turok, Phys. Rev. **D76**, 023501 (2007), hep-th/0612026.
- [23] K. Koyama and D. Wands, JCAP **0704**, 008 (2007), hep-th/0703040.
- [24] K. Koyama, S. Mizuno, and D. Wands, Class. Quant. Grav. **24**, 3919 (2007), 0704.1152.
- [25] C. Gordon, D. Wands, B. A. Bassett, and R. Maartens, Phys. Rev. **D63**, 023506 (2001), astro-ph/0009131.
- [26] J.-L. Lehners, P. McFadden, N. Turok, and P. J. Steinhardt, Phys. Rev. **D76**, 103501 (2007), hep-th/0702153.
- [27] A. J. Tolley and D. H. Wesley, JCAP **0705**, 006 (2007), hep-th/0703101.
- [28] J.-L. Lehners and P. J. Steinhardt, Phys. Rev. **D79**, 063503 (2009), 0812.3388.
- [29] J.-L. Lehners, P. J. Steinhardt, and N. Turok (2009), 0910.0834.
- [30] L. A. Boyle, P. J. Steinhardt, and N. Turok, Phys. Rev. **D69**, 127302 (2004), hep-th/0307170.
- [31] D. Baumann, P. J. Steinhardt, K. Takahashi, and K. Ichiki, Phys. Rev. **D76**, 084019 (2007), hep-th/0703290.
- [32] J. Khoury, B. A. Ovrut, P. J. Steinhardt, and N. Turok, Phys. Rev. **D66**, 046005 (2002), hep-th/0109050.
- [33] P. Creminelli, A. Nicolis, and M. Zaldarriaga, Phys. Rev. **D71**, 063505 (2005), hep-th/0411270.
- [34] D. H. Lyth, Phys. Lett. **B524**, 1 (2002), hep-ph/0106153.
- [35] A. J. Tolley, N. Turok, and P. J. Steinhardt, Phys. Rev. **D69**, 106005 (2004), hep-th/0306109.
- [36] P. L. McFadden, N. Turok, and P. J. Steinhardt, Phys. Rev. **D76**, 104038 (2007), hep-th/0512123.

- [37] J. Khoury and P. J. Steinhardt (2009), 0910.2230.
- [38] A. Linde, V. Mukhanov, and A. Vikman, JCAP **1002**, 006 (2010), 0912.0944.
- [39] F. Finelli, Phys. Lett. **B545**, 1 (2002), hep-th/0206112.
- [40] A. Notari and A. Riotto, Nucl. Phys. **B644**, 371 (2002), hep-th/0205019.
- [41] D. Langlois and F. Vernizzi, JCAP **0702**, 017 (2007), astro-ph/0610064.
- [42] J. Khoury, P. J. Steinhardt, and N. Turok, Phys. Rev. Lett. **91**, 161301 (2003), astro-ph/0302012.
- [43] J.-L. Lehners and N. Turok, Phys. Rev. **D77**, 023516 (2008), arXiv:0708.0743 [hep-th].
- [44] J.-L. Lehners and P. J. Steinhardt, Phys. Rev. **D78**, 023506 (2008), 0804.1293.
- [45] T. Battfeld, Phys. Rev. **D77**, 063503 (2008), 0710.2540.
- [46] C. T. Byrnes, M. Sasaki, and D. Wands, Phys. Rev. **D74**, 123519 (2006), astro-ph/0611075.
- [47] D. Babich, P. Creminelli, and M. Zaldarriaga, JCAP **0408**, 009 (2004), astro-ph/0405356.
- [48] J. M. Maldacena, JHEP **05**, 013 (2003), astro-ph/0210603.
- [49] K. Koyama, S. Mizuno, F. Vernizzi, and D. Wands, JCAP **0711**, 024 (2007), 0708.4321.
- [50] J.-L. Lehners and S. Renaux-Petel, Phys. Rev. **D80**, 063503 (2009), 0906.0530.
- [51] A. A. Starobinsky, JETP Lett. **42**, 152 (1985).
- [52] M. Sasaki and E. D. Stewart, Prog. Theor. Phys. **95**, 71 (1996), astro-ph/9507001.
- [53] D. H. Lyth, K. A. Malik, and M. Sasaki, JCAP **0505**, 004 (2005), astro-ph/0411220.
- [54] E. I. Buchbinder, J. Khoury, and B. A. Ovrut, Phys. Rev. Lett. **100**, 171302 (2008), 0710.5172.
- [55] J.-L. Lehners and P. J. Steinhardt, Phys. Rev. **D80**, 103520 (2009), 0909.2558.
- [56] J.-L. Lehners and P. J. Steinhardt, Phys. Rev. **D77**, 063533 (2008), 0712.3779.
- [57] K. M. Smith, L. Senatore, and M. Zaldarriaga, JCAP **0909**, 006 (2009), 0901.2572.
- [58] J. Khoury and F. Piazza, JCAP **0907**, 026 (2009), 0811.3633.
- [59] D. Seery and J. E. Lidsey, JCAP **0701**, 008 (2007), astro-ph/0611034.
- [60] N. Bartolo, E. Komatsu, S. Matarrese, and A. Riotto, Phys. Rept. **402**, 103 (2004), astro-ph/0406398.